JCEEA

Czasopismo Inżynierii Lądowej, Środowiska i Architektury

Journal of Civil Engineering, Environment and Architecture

Kwartalnik
tom XXXVI
zeszyt 66 (nr 1/2019)
styczeń-marzec

(e-ISSN 2300-8903)

Czasopismo Inżynierii Lądowej, Środowiska i Architektury jest kontynuacją
Zeszytów Naukowych Politechniki Rzeszowskiej - Budownictwo i Inżynieria Środowiska.

Issued with the consent of the Rector

Editor in Chief Publishing House of Rzeszow University of Technology
Professor Grzegorz OSTASZ, DSc, PhD

e-ISSN 2300-8903; p-ISSN 2300-5130

The electronic version of the Journal is an original version

Editorial Office: Rzeszow University of Technology, Faculty of Civil and Environmental Engineering and Architecture, St. Poznańska, 35-084 Rzeszów, Poland, www.oficyna.prz.edu.pl//pl/zeszyty-naukowe/czasopismo-inzynierii-ladowej-s/ (e-mail: jceea_bud@prz.edu.pl)

Publisher: Publishing House of Rzeszow University of Technology, 12 Powstanców Warszawy Ave., 35-959 Rzeszow, www.oficyna.prz.edu.pl (e-mail: oficyna@prz.edu.pl)

Additional information and an imprint – p. 69

Table of Contents

CZASOPISMO INŻYNIERII LĄDOWEJ, ŚRODOWISKA I ARCHITEKTURY
JOURNAL OF CIVIL ENGINEERING, ENVIRONMENT AND ARCHITECTURE
JCEEA, t. XXXVI, z. 66 (1/19), styczeń-marzec 2019, s. 5-15, DOI:10.7862/rb.2019.1

Kamila BOGUSZEWSKA[1]

SELECTED RESIDENCES IN THE ZAMOŚĆ ENTAIL – THE STATE OF PRESERVATION AND THE PROBLEMS OF PROTECTION OF THE ESTATES

The cultural landscape of the Lubelskie Region is a subject to irreversible changes. Urban transformation of the structure and architecture of the cities of the Lubelskie Region, the new character and organization of urban space, changes in ownership and subdivision of historical residences including historical parks, palaces and manors are the processes that take place in the space and landscape of the Lublin Voivodeship. The research paper concerns the area of the former Zamość Entail (the Zamoyski Family Fee Tail), which was founded in the Lublin area as early as in 16th century. The article presents the results of the survey of the architecture of the selected residences and their surrounding buildings. It focuses on the subject of protection and current state of preservation of the estates that constitute the cultural heritage of the Zamość Region.

Słowa kluczowe: historical residences, Lublin region, cultural hertige

1. Introduction

The historical residences have become the inseparable part of the cultural landscape of the Lubelskie Region constituting the cultural and historical heritage of the province. The land estates destroyed and ravaged during the World War II and parcelled after 1944 were later adapted to fulfil different functions. Their fates have varied. However, the main goal of the socialist regime in Poland was to completely discredit the gentry. Therefore, the palaces and manors were being transformed into tuberculosis hospitals (Adampol, Gościeradów), psychiatric hospitals (Łysołaje), orphanages (Czemierniki), agriculture schools (Kijany, Jabłoń, Stryjów), welfare homes (Klemensów, Kock etc.). Historical stands were cut down and sport fields were introduced into the parks (Lubartów, Zawieprzyce, Kijany). Old farm buildings were usually taken over by State Collective Farms (in Polish: PGR) until the end of 90-ties of the 20th century. Smaller and medium residences were demolished or adapted into apartments of former farm workers

[1] Kamila Boguszewska. Samodzielna Pracownia Architektoniczna, Lublin University of Technology, Faculty of Civil Engineering and Architecture, Nadbystrzycka 40, 20-618, Lublin, Poland, k.boguszewska@pollub.pl

(Siedliszczki), smaller health centres (Kanie, Surhów, Samoklęski, Krzesimów) or schools (Brzezice, Chojeniec, Sielec). It is estimated that in the 20th century about 200 of those buildings ceased to exist – half of them were destroyed before the World War II and 30% of them disappeared in the last half of the century [1].

This article is to outline the subject of the selected residences of the former Zamość Entail against the background of the processes and actions taking place over the last 70 years in the Lublin Voivodeship, and also the state of preservation and problems of the protection of such buildings.

2. The contemporary state of research

The subject of historical residences, especially of the manors of the Lubelskie Region, their state of preservation, architectural form, construction materials and construction was the topic of studies that were conducted at the end of the 1970s and in the 1980s. The scientist who was working on the subject of the wooden manors in the Lubelskie Region was R. Brykowski (1981), co-author of the multi-volume publication *The monuments of architecture and construction in Poland - Zabytki architektury i budownictwa w Polsce* (1984 – 1999). Smaller residences of the gentry were also the subject of the work of J. Petera (1978). In her paper she tried to catalogue preserved and already inexistent residences. Over time, her work was supplemented with the findings of other researchers, among the others J. Górak, the author of the article *Unknown manors of the Lubelskie Region* (*Nieznane dworki Lubelszczyzny* - 1986) and the article which has updated existing knowledge of the subject at the end of 20th century: *Of the causes of the architecture of manors in the Lubelskie Region (O przyczynkach architektury dworów Lubelszczyzny)*.

The state of preservation of the farm complexes accompanying manors and palaces of the Lubelskie Region was the subject of research of B. Kwiatkowski. He embodied his discoveries in the paper, and then monograph: *The farm complexes of the Lubelskie Region: the history of the development and construction* (*Folwarki Lubelszczyzny: historia rozwoju i zabudowy – 2012)*. Historical parks were the subject of research of M. Kseniak (1981, 1982) and D. Fijałkowski (1982). Nowadays the substantial source of information concerning statistical data on the state of preservation and the way of use of the residential architecture of the Lubelskie Region are the reports of the National Heritage Institute (2017) made within the framework of the National Program for the Protection of Monuments and Care of Monuments for 2014 – 2017 [2].

3. The situation and quantity of historical residences in the Lublin voivodeship

The biggest concentration of the estates in the Lublin Voivodeship is in the belt between Kazimierz Dolny and Tomaszów Lubelski. It was the area where most of the larger and medium residential complexes were founded [3].

This region is also full of aristocratic residences of trans-regional importance like palace complexes in Kock, Opole Lubelskie, Puławy, Radzyń Podlaski or historical residences in the area of the current Zamość poviat – a part of the area of the former Zamość Entail that is the palace in Łabunie founded by Jan Jakub Zamoyski [4] and the summer residence in the Zamoyski Family Fee Tail in Michałów – Klemensów [2]. According to D. Fijałkowski, an the beginning of the 20th century, the number of manors and farm estates in the area of the Lubelskie Region was estimated at 650 [5],[6]. Interestingly, according to J. Górak, the total number of manors, both bricked and wooden was 895, including 234 unrecognized buildings [7]. It's true that a part of the residences of cotters of the farm complexes had the architectural form of country manor, which made them the part of the unrecognized buildings [13].

Nowadays there are 416 buildings in the register of monuments in the area of the Zamość poviat including the Zamość city – the family seat of Zamoyski Family Fee Tail, the city considered as a monument of history. It consists of 16 buildings classified as residential architecture, 37 as historical greenery (parks surrounding manors and palaces) and cemeteries. Twenty-six buildings were former farm complexes.

Nowadays in the collections of the National Heritage Institute, there is documentation of 463 park complexes of the Lubelskie Region, which is 6.22% of the whole number of these facilities in Poland. Historical residences are estimated at 267, so 5.51%, and farm complexes at 307, so 5.71% of the total number for the whole country. The number industrial facilities of the Lublin Voivodeship is most modest: only 71 buildings – 2.71% of the total stock in Poland [2]. It's worth to mention that most of palaces and manors that survived till this day in the Lubelskie Region are in the register of the Lublin's Office of Monuments Protection. The above-mentioned greenery was always connected with palace and manor complexes. A part of it is only one remaining trace of the former residences [2].

4. Zamoyski family fee tail

Zamoyski Family Fee Tail (in Polish: Ordynacja) was established in 1589 with the decision of the general sejm in Warsaw. The founder of the fee tail was Jan Zamoyski, Great Crown Chancellor and Great Crown Hetman. Emerge of the territorial power in the south part of the Lubelskie Region was started by Jan Zamoyski with four villages inherited from his father, Stanisław Zamoyski: Skokówka, Zdunów, Kalinowice and half of the Pniówek village. Apart from this area, two cities were included in the statute of the fee tail: Zamość and Tarnogród. In four years, szczebrzeskie, turobińskie, gorajskie and kraśnickie estates were joined to the Zamoyski Family Fee Tail. Over the years, the fee tail was becoming bigger and bigger and at the beginning of 17th century it has 3 710 km^2. [8]

In 1772, there were 189 villages in the area of the Zamość State; 30 years later – 221 [9]. The basis of the economics of the fee tail was agriculture based on the system of farm complexes. At the end of 18th century, it was already 97 farm complexes and more modest residences being their part and belonging to the Zamoyski family [8].

In 19th century, the Zamoyski Family Fee Tail consisted of 9 cities, 291 villages and 116 farm complexes. The surface of the fee tail was 373,723 ha, and it was populated by 107,764 people [6].

The residences of the bailiffs of farm complexes of the Zamoyski Family Fee Tail have differed in terms of architecture from usual residences of the owners and cotters of farm complexes. They often had the architectural form of the country manor, and after subdivision, they were becoming the residences of their cotters [13]. Many times they had the form of palaces or villas like already inexistent palace in Łukowa. Apart from the residences like palace in Klemensów, Łabunie, they were an inseparable element of the landscape of the area of the Zamoyski Family Fee Tail (Fig. 1).

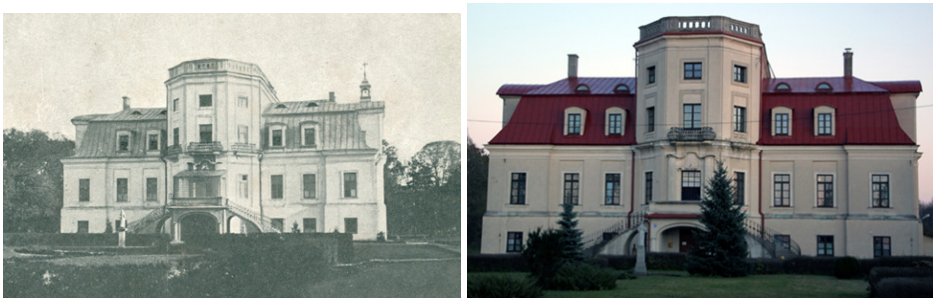

a) b)

Fig. 1. The palace in Łabunie 1897-1944 (a) ; the palace in Łabunie, current state (b), fot. the author

The article presents three selected residences of such type: we will begin with the palace – park complex in Klemensów and then we will discuss much smaller manors in Sól and Łukowa, which were the residences of the cotters of farm complexes of the Zamoyski Family Fee Tail.

5. Palace – park complex in Klemensów

One of the most representative seats of the Zamoyski family was doubtlessly the summer residence in Klemensów situated in the area of Bodaczów village near Zamość by the Wieprz river.

The construction of the palace started in 1740 thanks to the 7th Ordynat - Tomasz Zamoyski. It was meant to be used as place of recreation for the future 8th Ordynat – Klemens, son of Tomasz, who has suffered from recurring health problems. Construction of the palace has been surveyed by genial engineers and

architects, for example engineer Jan Andrzej Bem, architect Henryk Ittar, Jerzy de Kawe or constructor J. Columbani [10].

The building of the surface of 3000 m^2 was situated in the landscape park, which was extended by the following Ordynats in the English style. After the war, the palace was used as an orphanage (1944 – 1966), and afterwards until 2006, by Social Home run by the Sisters of St. Francis. From the beginning of 2018, the palace – park complex in Klemensów returned to the Zamoyski family. The estate of total surface of 136.62 ha is situated on 12 plots. In 2016, the Zamoyski family requested the return of the estate in Klemensów. The Lublin Voivode agreed to sell the estate to the applicants. The Zamoyski family got a discount of 99.1% of the property value. The palace – park complex of estimated value of 7.3 mln zł was sold for 87 thousand zł, provided that if during 10 years the Zamoyski family decided to sell the property, they would have to pay back the discount to the state [11].

Currently, there are renovation and cleaning works at the palace and its surroundings (Fig. 2–4).

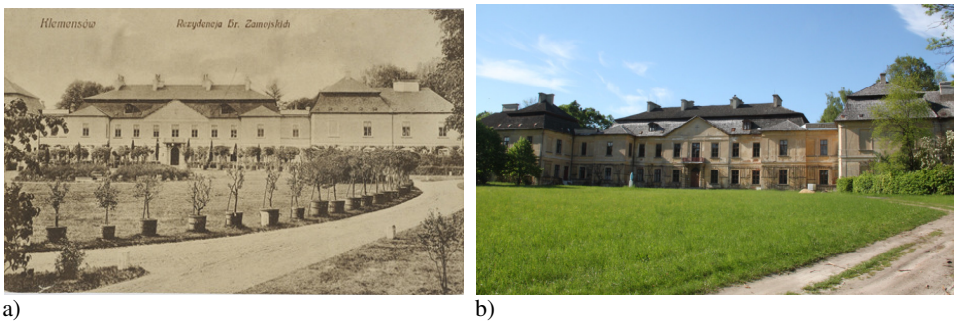

a) b)

Fig. 2. The palace in Klemensów at the beginning of 20th century (a) ; the palace in Klemensów – current state (b), fot. the author

Fig. 3. The palace in Klemensów – current state, fot. the author

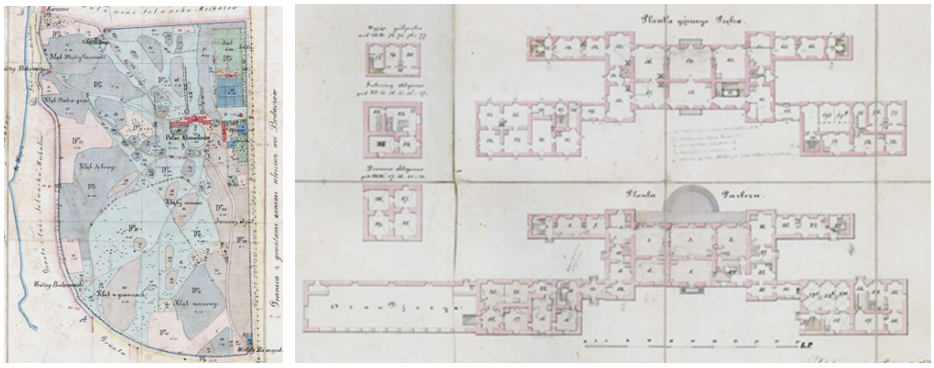

a) b)

Fig. 4. The plan of the park and palace in Klemensów in 1872 APL, AOZ (a-b)

6. The farm complex in Sól

The palace - park complex in Sól is a perfect example of the complex that as a matter of fact has returned to the original owners – Rączyński and Kiełczewski family – but still it was demolished in 1944 – 1950 because of its bad technical condition. Construction materials from the demolition were sold to the local residents who used them to build their own houses.

The farm complex was situated in Biłgoraj commune and was the part of the farm complexes of the Zamość Entail. After parcelling of the property in 1923, it became the possession of Józef Kiełczewski, and since 1935, of Franciszek Rzączyński.

The surface of the farm complex was then 500 hectares of farmlands and 150 hectares of fields. The complex consisted of half-hectare fruit – vegetable garden and three water reservoirs. The Dąbrowica river was flowing by the farm complex. During the World War II, the river course was changed, when the Germans adapted the property in Sól to horticulture farm and cut down the historical alley leading to the manor [12].

The manor in Sól was probably built in the second half of the 19th century. It was laid out on the elongated, rectangular plan. The ten-axis building with irregular window openings disrupted with later extensions was erected solely from the blanched wood based on the brick foundation. The body of the building was covered with wood shingles and partly with tar roofing felt. The characteristic feature was portico on the south-west façade being the front façade of the building. It was based on four columns [13]. Even in surveys concluded in the 1920s, the technical condition of the building was defined as "*passable*". Apparently already at that time, the secondary layers disrupting the original form of the manor in the form of the attached bay window and the elements that needed to be changed like crooked wooden columns supporting the arcades were clearly visible (Fig. 5, Fig. 6, Fig. 7B).

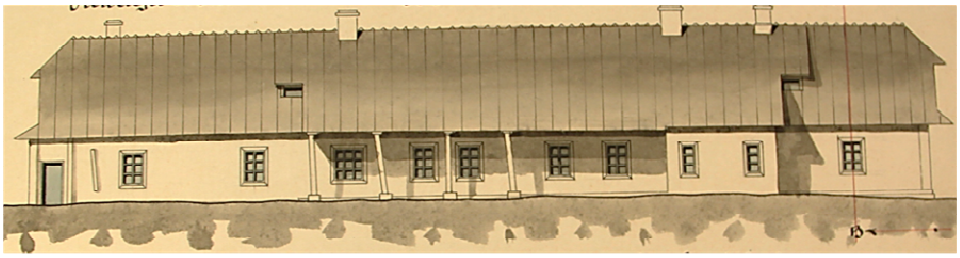

Fig. 5. The front facade of the manor in Sól, the survey of 1922, APL, AOZ, p.

Inside the manor, there were fifteen enfiladed rooms. In the place of the dismantled manor, at the efforts of the Rączyński family, a new residential building was erected in the 1990s. The form of the new building doesn't correspond with the architectural form of the historical seat of the cotter of the farm complex.

The manor was accompanied with a fruit and vegetable garden situated on the north-west side. From the southeast, it bordered on the stable, and from the southeast, on the wooden house of the writer and gardener of the farm complex. The plan of the garden hasn't survived till this day. Pictures from 20th century shows flower beds and flower compositions with exotic plants in the pots in most exposed places of the park like for example flowerbeds in Sól (Fig. 7B).

Fig. 6. Ewa and Józef Kiełczewscy against the background of the manor with the arcade (the archive of The "Grodzka Gate – NN Theatre" Centre)

a) b)

Fig. 7. Anna Rzączyńska, Róża Libek, Juliusz Libek in Sól (the archive of The "Grodzka Gate – NN Theatre" Centre) (a); Planting of flowers in Sól (the archive of The "Grodzka Gate – NN Theatre" Centre) (b)

7. The farm complex in Łukowa

There is not even a remaining trace of the former farm complex in Łukowa, which was belonging to the Zamoyski Family Fee Tail. In the 19th century, the manor area of Łukowa was partly in the Zamoyski Family Fee Tail and partly private property [14]. Back then there were the starost's farm complex and two ponds [15]. The palace being the residence of the cotter of the farm complex didn't survive the World War II turbulences. One and only iconographic material that survived until this day is the survey of the building from the 1920s.

The architectural form of provincial, eclectic building corresponded with palaces and villas erected by Teodor Talowski – architect who was in vogue back then. Palace was built of brick based on the plan of sculptural rectangle with numerous bay windows, which were entrances to the building. The front façade (from the southeast) was highlighted with representative portal. The building was dominated by a three-storey tower in the southwest part of the palace with a streamer with possible date of the construction – 1906 (Fig. 8). From the north-east side, in the middle of the façade, there was a wooden porch with three steps leading to a garden. The roof of the building was covered with two-color cement roof tiles. The rooms were aligned with one another in enfilade, and in the ground floor, apart from kitchen and bedrooms with the direct entrance from the garden, it was small winter garden with characteristic big window closed with an arc.

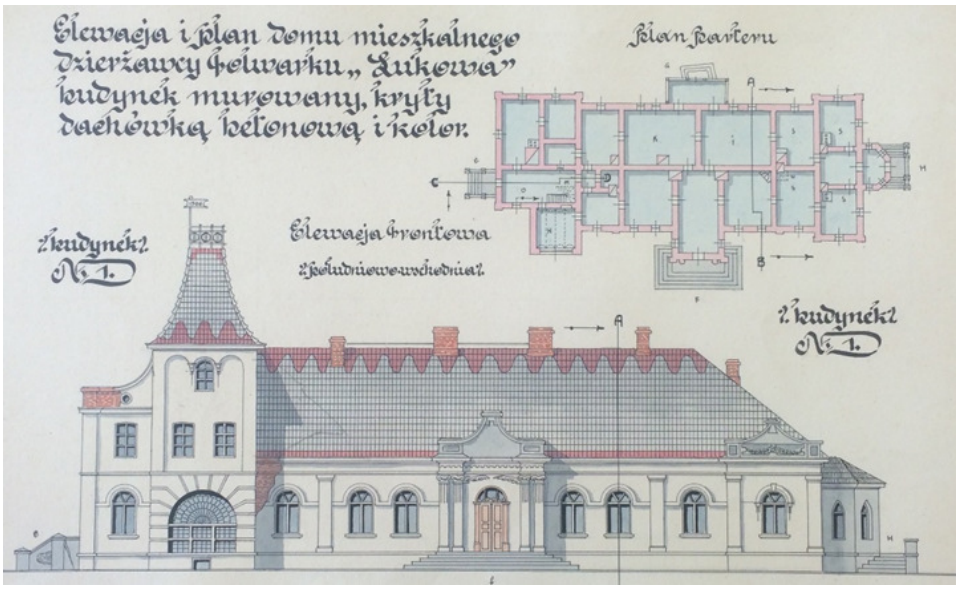

Fig. 8. The front façade of the manor in Łukowa, the survey from 1922, APL, AOZ

8. The hazards and state of preservation

The article has discussed three selected historical residences in the Zamość area. As we can see, their fates have varied. Only one of the presented buildings has survived till this day: the palace – park complex in Klemensów. It's a because this building was always in use, and on-going maintenance works were conduced, although not always in accordance with the good engineering practice. Despite the fact that the building was redeveloped and adapted by then authorities, the palace stayed in quite good shape. The fact that the original owners retrieved it gives hope that it will be restored to its former glory.

Two remaining buildings (the manors in Łukowa and in Sól) didn't survive war and after-way period. It's worth mentioning that significant portion of historical manors was destroyed especially in 1950s and 1960s as the symbol of fight with then eliminated gentry. It's true that it was possible to save many of those buildings. Unfortunately, a part of them was dismantled and used for cheap construction material by local residents and a part of them was dismantled because of the "bad technical condition".

In 1983, the number of survived manors in the former Zamość Voivodeship was 29 – on the turn of 1960s and 1970s 21 manors were demolished, and until 1945 – 15 [16]. After 1945, the manor in Antonówka (demolished in 1960), Baranica (demolished in 1961), Bzowiec Dolny or Chomęciska Małe (manor demolished in 1960) disappeared from the area of the former Zamość Voivodeship. Construction materials taken from the demolition were used for

example to build a fire station and new residential buildings. A similar fate was shared by other manors, for example the one in Grabowczyk, which was finally demolished in 1965, Honiatycze, Horyszór Ruski – demolished in 1946, Kryniczki, Nielisz – demolished after 1945, Pularzów – demolished in 1977 and Skierbieszów – demolished after 1950, etc. [3].

Taking into consideration the newest rapport of the National Heritage Institute, the state of preservation of the residential architecture of the Lubelskie Region is on the third place just after industrial buildings and farm complexes which disappears at an alarming rate (these buildings constitutes today 5.59%; so 17 buildings at stake out of 304 in the whole Lublin Voivodeship). Residential architecture on the line constitutes 4.17%, so 11 buildings out of 264 of the whole stock. The biggest threats for the historical buildings are wear and tear of the materials / construction (46 buildings), no resident (27 buildings) or no proper protection and on-going conservation (24 buildings) [2].

Unfortunately, there is no bright future for the residential architecture. Complicated proprietary issues and often no physical presence of the owner really hinder implementation of necessary repairs and renovations. One of the possible solutions to save historical residences is their conscious adaptation and conservation with the use of the UE funds.

References

[1] B. Stanek-Lebioda, Zachowane dwory ziemiańskie Lubelszczyzny – nie wszystko minęło, [in:] Ziemiaństwo na Lubelszczyźnie, The materials from the scientific session organized in the Zamoyski Museum in Kozłówka, elaborated by Róża Maliszewska, the Zamoyski Museum in Kozłówka, (2001), p. 100.

[2] Raport o stanie zachowania zabytków nieruchomych w województwie lubelskim, Zabytki wpisane do rejestru zabytków – The report of the state of preservation of the monuments in the Lublin Voivodeship (A and C register volumes), Warszawa, (2017), p. 30, 31, 34, 59–63.

[3] J. Petera, Wiejskie dworki drewniane na Lubelszczyźnie, [in:] Z Zagadnień Kultury Ludowej, T.,(1978), p. 177–179, 90–155.

[4] The design of the palace is associated to Bernard Merytyn [after:] J. Kowalczyk, Zainteresowania i działalność architektoniczna Ordynatów Zamoyskich XVIII wieku, [in:] Ziemiaństwo na Lubelszczyźnie, Materials from the 2nd scientific session organized in the Zamoyski Museum in Kozłówka, 22-24 May 2002, the Zamoyski Museum in Kozłówka, (2003), p. 104.

[5] D. Fijałkowski, M. Kseniak, Parki wiejskie Lubelszczyzny, Stan ochrona i rewaloryzacja biocenotyczna, Warszawa, (1982), p. 36.

[6] B. Kwiatkowski w publikacji Folwarki Lubelszczyzny: historia rozwoju i zabudowy, Lublin: Politechnika Lubelska, (2012), p. 7, 68 it is estimated that in the turn of 19th and 20th century the number of manors and farm complexes in the Lubelskie Region was 645 and the rotation of the owners was 50%.

[7] J. Górak, Przyczynki do architektury dworów na Lubelszczyźnie, {in:} Ziemiaństwo na Lubelszczyźnie, Materials from the 2nd scientific session organized in the

Zamoyski Museum in Kozłówka, 22-24 May 2002, the Zamoyski Museum in Kozłówka, (2003), p. 236. In this article Jan Dworak presented table with results of the survey on the number of bricked and wooden manors – 425, inexistent – 236 and unrecognized – 234.

[8] M. Kowalski, Państwo magnackie w strukturach polityczno – administracyjnych Rzeczpospolitej Szlacheckiej na przykładzie Ordynacji Zamoyskiej, in: Przegląd geograficzny, (2009, 81,2), p. 182–184, 186.

[9] M. Kozaczka, Ordynacja Zamojska 1919–1945, Norbertinum, Lublin, (2003), M. Kozaczka, *Poczet Ordynatów Zamoyskich,* Norbertinum, Lublin, (2004).

[10] D. Kawałko, Klemensów zespół pałacowo – parkowy, Biuro badań i dokumentacji zabytków, Zamość, (1986), p. 7.

[11] A. Ciurysek, Zamoyscy znów w pałacu, [in:] Nowy Kurier Zamojski, 14.03.2017

[12] http://teatrnn.pl/leksykon/artykuly/ziemianstwo-na-lubelszczyznie-majatek-sol/, acces: 29.06.2018.

[13] J. Petera, Nieznane i zapomniane dworki drewniane na Lubelszczyźnie, Ziemiaństwo na Lubelszczyźnie, Muzeum Zamoyskich w Kozłówce, (2001), p. 126.

[14] Słownik Geograficzny Królestwa Polskiego i innych krajów słowiańskich, edited by F. Sulmirski, B. Chlebowski, W. Walewski, Vol. V, Warszawa, (1880), p. 824–825.

[15] http://www.lukowa.pl/index.php/historia-lukowej, access: 29.06.2018.

[16] J. Górak, Nieznane dworki Lubelszczyzny, Studia i Materiały Lubelskie, (1986), Vol. 11, 177–179.

Przesłano do redakcji: 20.09.2018 r.

CZASOPISMO INŻYNIERII LĄDOWEJ, ŚRODOWISKA I ARCHITEKTURY
JOURNAL OF CIVIL ENGINEERING, ENVIRONMENT AND ARCHITECTURE
JCEEA, t. XXXVI, z. 66 (1/19), styczeń-marzec 2019, s. 17-26, DOI:10.7862/rb.2019.2

Dorota SZAL[1]
Renata GRUCA-ROKOSZ[2]

ANAEROBIC OXIDATION OF METHANE IN FRESHWATER ECOSYSTEMS

Anaerobic oxidation of methane (AOM) is a biochemical process that plays an important role in aquatic ecosystems, as it significantly reduces the emission of methane (CH_4) to the atmosphere. Under anaerobic conditions, CH_4 can be oxidized with electron acceptors, such as sulphates (SO_4^{2-}), nitrates (NO_3^-) or nitrites (NO_2^-), iron (Fe^{3+}), manganese (Mn^{4+}) and humic substances. The anaerobic oxidation of methane is mainly regulated by anaerobic methanotrophic archaea (ANME) and sulphate reducing bacteria. The AOM process is crucial to understand the CH_4 cycle and anticipate future emissions of the gas from water reservoirs. The process is widely described in marine environments, however very little is known about its occurrence and importance in freshwater systems. There is a great demand for this kind of the research, especially in ecosystems exposed to long-term anaerobic conditions, which may be in degraded reservoirs.

Keywords: anaerobic oxidation of methane, electron acceptors, methanotrophic archaea

1. Introduction

Methane (CH_4) is a gas emitted to the atmosphere from both natural and anthropogenic sources. It contributes to the greenhouse effect and global climate change [24]. Production of CH_4 occurs under anaerobic conditions with the participation of metanogenic archaea; in turn, methane oxidizing bacteria (metanotrophic archaea) contribute to reducing the emission of this gas to the atmosphere. Although aerobic methane-oxidizing bacteria (MOB) have been known for over 100 years [60], it was only at the turn of the last century that organisms involved in anaerobic oxidation of methane (AOM) were identified. Anaerobic methanotrophic archaea (ANME) are of great importance in regulating the Earth's climate, because they reduce the emission of large

[1] Corresponding author: Dorota Szal, Politechnika Rzeszowska, ul. Powstańców Warszawy 6, 35-959 Rzeszów, d.piwinska@prz.edu.pl
[2] Renata Gruca-Rokosz, Politechnika Rzeszowska, ul. Powstańców Warszawy 6, 35-959 Rzeszów, renatagr@prz.edu.pl

amounts of CH_4 accumulated in bottom sediments [32]. The process of anaerobic oxidation of methane (AOM) is widely described in marine environments, however very little is known about its occurrence and importance in freshwater systems [8; 26]. Just a decade ago, sulfates were the only known electron acceptor supporting anaerobic oxidation of methane [32; 38]; however, there are many other electron acceptors in the environment, such as: iron (Fe^{3+}), manganese (Mn^{4+}), nitrates (NO_3^-) [19] or nitrites (NO_2^-) [14; 48], which are thermodynamically more preferred than sulfates.

2. Anaerobic oxidation of methane

Methane emission from sediments is the net result of two processes: methanogenesis, which occurs in the hypoxic part of bottom sediments, and the oxidation of CH_4 as a result of aerobic or anaerobic microbiological processes [42]. AOM is an important process in marine and freshwater ecosystems [33; 44; 45], because it plays a key role in reducing the flow of CH_4 from bottom sediments to the overlying water, and thus also to the atmosphere [5; 34; 37]. AOM mainly occurs in the presence of methanotrophic archaea and sulfate-reducing bacteria [7]. AOM plays an important role in controlling CH_4 emissions in marine sediments, where it is oxidized on average 300–380 Tg $CH_4 \cdot yr^{-1}$ [20; 46]. It has also been estimated that, for example, in wetlands the AOM process can consume 4.1-6.1 Tg $CH_4/m^2 \cdot yr$, which is about 2-6% of the CH_4 emissions from wetlands in the world [23]. In the absence of oxygen, microorganisms can oxidize CH_4 in the presence of alternative electron acceptors, such as: sulfates, nitrates, nitrites, iron, manganese and humic substances [6; 7; 9; 14; 15; 18; 19; 21; 39; 45; 48; 49; 54; 56; 63].

Anaerobic oxidation of methane coupled with sulfate reduction (AOM-SR) is the main process contributing to a significant reduction of methane produced in marine sediments. AOM-SR is regulated by a consortium of anaerobic methanotrophic archaea (ANME) and sulfate-reducing bacteria [32]. Methane is oxidized according to reaction:

$$CH_4 + SO_4^{2-} \rightarrow HCO_3^- + HS^- + H_2O \quad (1)$$

The AOM-SR process is influenced by the distribution of CH_4 and SO_4^{2-} in bottom sediments [26], as well as the stable isotopic composition $\delta^{13}C\text{-}CH_4$ [1]. There is little evidence of the role of this process in freshwater sediments, where the reduction of sulfate is limited. However, the results of the research presented in some publications [42; 51] indicate that AOM-SR can play a significant role in regulating the flow of CH_4 from sediments for SO_4^{2-} concentrations typical for freshwater reservoirs. AOM dependent from SO_4^{2-} concentrations have been demonstrated in the bottom sediments of Lake Cadagno (Switzerland) based on the isotopic analysis of carbon and archaea involved in the AOM. This process

was particularly present near the surface of the sediment, where the concentration of SO_4^{2-} was > 2 mmol/l [52]. In turn, based on the research of some authors [42; 51], it was concluded that in a monomictic lake in Denmark (lake Ørn) high concentrations of sulfates may adversely affect the thermodynamics of the AOM process. Therefore, further research is needed to quantify the role of AOM in the CH_4 cycle in various freshwater environments.

Electron acceptors, i.e. nitrates, nitrites, iron and manganese, may play a potentially greater role in freshwater ecosystems [42]. Due to the fact that SO_4^{2-} concentrations are generally at low level in freshwater lakes, NO_3^- and NO_2^- may play a greater role in the AOM process. If nitrates and/or nitrites are available in anaerobic sediments, anaerobic bacteria oxidizing nitrates and/or nitrates take part in the AOM process. In this case, CH_4 can be used as an electron donor (reactions 2 and 3) [62], and sulfate reduction usually does not occur [50]. This process is called anaerobic oxidation of methane coupled with denitrification (AOM-D) [11; 41].

$$3CH_4 + 8NO_2^- + 8H^+ \rightarrow 3CO_2 + 4N_2 + 10H_2O \quad (2)$$

$$CH_4 + 4NO_3^- \rightarrow CO_2 + 4NO_2^- + 2H_2O \quad (3)$$

The AOM-D process is thermodynamically more favorable than AOM-SR. Therefore, AOM-D has become the subject of many scientific studies [14; 25; 45]. AOM-D was observed in lake sediments with a high concentration of NO_3^- [12; 37].

It is also possible to oxidize CH_4 by reducing manganese (Mn) or iron (Fe) (reactions 4 and 5) as confirmed by recent studies [6; 10; 53].

$$CH_4 + 4MnO_2 + 7H^+ \rightarrow HCO_3^- + 4Mn^{2+} + 5H_2O \quad (4)$$

$$CH_4 + 8Fe^{3+} + 2H_2O \rightarrow CO_2 + 8Fe^{2+} + 8H^+ \quad (5)$$

In the environment, iron reduction is often limited by the bioavailability of iron oxides, as iron (III) or complex iron compounds are not commonly found. In the publication of Ettwig et al. [17], the enrichment culture was incubated with more available metal forms: nanoparticle ferrihydrite (Fe^{3+}) and birnessite (Mn^{4+}). Selected electron acceptors supported the oxidation of CH_4 to CO_2, although the process itself was at a lower rate compared to nitrates and Fe (III) as iron citrate as electron acceptors. Stimulation of AOM after the addition of oxidized forms of Mn or Fe was observed in laboratory incubations of SO_4^{2-}–depleted freshwater sediments. It was found that iron reduction affects AOM in lake sediments, as indicated by higher $\delta^{13}C$-CH_4 values in deeper sediment layers [53]. AOM coupled with reduction of Mn and/or Fe was also observed in the water column of thermally stratified Lake Matano (Indonesia), the world's largest known ferruginous reservoir [10]. These studies have shown that the role

of Mn and Fe oxides in AOM is indirect and involves the stimulation of oxidative sulfur circulation, which can supply SO_4^{2-} to AOM-SR. Based on the study of lake Ørn sediments (Denmark), it was concluded that the process took place at significant depths, where both iron and sulfates were present in low concentrations, confirming the significance of AOM-Fe/Mn in Fe/Mn–depleted sediments. Furthermore, anaerobic reduction of iron (Fe^{+3}) and manganese (Mn^{+4}) coupled with AOM is regarded as more favorable process; and it has been shown that it is a significant process in lakes [42; 53]. Little is known about the microorganisms involved in AOM-Fe/Mn. However, on the basis of the conducted research [6], it was noticed that a large group of microorganisms of AOM-Fe/Mn in sediments after incubation were microorganisms associated with the marine benthic Archaea group D and ANME [42].

The rate of anaerobic oxidation of CH_4 depends not only on the availability and concentration of anaerobic oxidants, but also on the weather conditions and physical factors prevailing on the reservoir, such as water turbulence [3; 31]. High wind speeds can lead to complete mixing of the reservoir waters in a short time, e.g. in autumn . Therefore, the majority of CH_4 can be emitted to the atmosphere due to increased transport through different water layers and a short residence time in the water column [3; 29]; on the other hand, gradual mixing of reservoir water may cause that CH_4 will be longer available for bacteria participating in AOM [29], which will reduce its emission to the atmosphere.

3. Anaerobic methanotrophic archaea

Anaerobic methanotrophic archaea (ANME) are involved in anaerobic methane oxidation – in the process opposite to methanogenesis [32]. Based on the phylogenetic analysis of the 16S rRNA gene, ANME were divided into three groups: ANME-1, ANME-2 and ANME-3 [8; 21; 33; 40]. All ANMEs are phylogenetically linked to various groups of methanogenic archaea. ANME-2 and ANME-3 belong to the order *Methanosarcinales*; in turn, ANME-1 belong to the order related to *Methanosarcinales* and *Methanomicrobiales* [32]. ANME-3 are closely related to the *Methanococcoides* gene. Microorganisms belonging to the ANME-2 and ANME-3 groups have a shape similar to methanogens of *Methanosarcina* and *Methanococcus*; whereas ANME-1 show a different morphology. ANME strains occur in anaerobic freshwater sediments, as well as in marine environments, aquifers and soils [32; 58].

AOM-SR is a metabolic process combined with SO_4^{2-} reduction, obtaining energy through syntrophic consortium of the ANME and sulfate reducing bacteria (SRB) [7; 22]. Some SRB groups: *Desulfosarcina*/*Desulfococcus* and *Desulfobulbaceae* participate in the sulfate reduction (SR) process together with ANME. However, it has been shown that some ANME filotypes perform SR without the presence of SRB in various aquatic environments [2; 35; 36; 59; 61], suggesting that AOM-SR may occur regardless of the occurrence of ANME [38].

In addition, Ettwig et al. [14] showed that AOM can be mediated via *Candidatus Methylomirabilis oxyfera* (NC10 type) in the presence of NO_2^-. The bacterium can produce oxygen by reducing NO_2^- and use the O_2 to oxidize CH_4 [11; 14]. *Methylomirabilis oxyfera*, an NC10 bacterium, and *Candidatus Methanoperedens nitroreducens*, ANME archaea, have been identified as microorganisms capable of carrying out AOM-D [14; 19; 37]. Denitrification metanotrophs seem to be common in freshwater sediments, as determined by 16S rDNA studies [16], but the quantitative role of NO_3^- or NO_2^- in AOM under natural conditions has not been studied so far.

AOM associated with the reduction of soluble iron complexes have recently been observed in environments rich in ANME-2 [49], and AOM coupled with reduction of iron or manganese oxides has been confirmed several times and presented in many scientific publications [6; 13; 43; 47; 53]. In addition to the ability of these bacteria to carry out AOM along with iron reduction in enrichment cultures [17], it was found that ANME-2d or AAA (*AOM-associated archaea*) containing *Candidatus Methanoperedens nitroreducens* carry out AOM-SR in the sediments of the alpine lake Cadagno (Switzerland) [52; 57]. Recent studies have concluded that the strain closely related to *Candidatus Methanoperedens nitroreducens* from freshwater enrichment culture is present during AOM coupled with the reduction of soluble and nanoparticulate iron forms [17].

Methane oxidizing bacteria not only reduce atmospheric CH_4 emissions, but also provide adequate nutrients for aquatic consumers [27]. In several scientific publications [4; 28; 30; 55] the role of CH_4 oxidizing bacteria was examined as a carbon source for zooplankton in humic lakes with thermal stratification of water. Kankaala et al. [30] showed that metanotrophs were a source of nutrients for a typical pelagic zooplankton – Daphnia. The authors also suggested that carbon from CH_4 plays a greater role in the trophic network of lakes than it was previously estimated.

4. Summary

Freshwater ecosystems are identified as one of the main natural sources of methane, but little is known about the importance of anaerobic methane oxidation (AOM) in these ecosystems. The emerging publications of many authors show that AOM can significantly reduce methane emissions from freshwater sediments. The study of the activity of microorganisms taking part in AOM and the ongoing metabolic processes with the participation of electron acceptors (Fe^{3+}, Mn^{4+}, SO_4^{2-}, NO_3^-, NO_2^-) is crucial in understanding the circulation and predicting future CH_4 emissions. The flow of methane into the atmosphere from aquatic ecosystems is regulated by two main groups of microorganisms. Methanogenic archaea are responsible for the production of CH_4, while methane-oxidizing bacteria (ANME) are responsible for the

consumption of CH_4 in these ecosystems. Different electron acceptors contained in sediments affect the presence of various groups and species of microorganisms characteristic of individual processes: AOM-SR, AOM-D and AOM-Fe/Mn. In marine environments, the dominant process is AOM coupled with sulfate reduction. In freshwater ecosystems, this process is probably limited by low sulfate concentrations. The methane oxidation processes associated with the reduction of alternative electron acceptors such as: nitrates/nitrites, manganese and iron are more significant there.

The work was supported by National Science Centre Poland, via grant no. 2017/25/B/ST10/00981.

References

[1] Alperin M.J., Reeburgh W.S., Whiticar M.J., Carbon and hydrogen isotope fractionation resulting from anaerobic methane oxidation, Global Biogeochem. Cycles, 2, 1988, 279–288.

[2] Aquilina A., Knab N.J., Knittel K., Kaur G., Geissler A., Kelly S.P., Fossing H., Boot C.S., Parkes R.J., Mills R.A., Boetius A., Lloyd J.R., Pancost R.D., Biomarker indicators for anaerobic oxidizers of methane in brackish-marine sediments with diffusive methane fluxes, Organic Geochemistry 41, 2010, 414–426.

[3] Bastviken D., Cole J.J., Michael L. Pace Matthew C. Van de Bogert, Fates of methane from different lake habitats: Connecting whole-lake budgets and CH_4 emissions, Journal of geophysical research, 113, 2008, doi:10.1029/2007JG000608.

[4] Bastviken, D., Ejlertsson, J., Sundh, I., Tranvik, L., Methane as a source of carbon and energy for lake pelagic food webs, Ecology 84, 2003, 969–981.

[5] Bastviken D., Ejlertsson J., and Tranvik L., Measurement of methane oxidation in lakes—A comparison of methods, Environ. Sci. Technol., 36, 2002, 3354–3361.

[6] Beal E.J., House C.H., Orphan V.J., Manganese- and Iron-Dependent Marine Methane Oxidation, 325(5937), 2009, 184–187, DOI: 10.1126/science.1169984.

[7] Boetius A., Ferdelman T., Lochtea K., Bacterial activity in sediments of the deep Arabian Sea in relation to vertical flux, Deep Sea Research Part II: Topical Studies in Oceanography, 47(14), 2000a, 2835–2875.

[8] Boetius A., Ravenschlag K., Schubert C. J., Rickert D., Widdel F., Gieseke A., Amann R., Jørgensen B. B., Witte U., Pfannkuche O., A marine microbial consortium apparently mediating anaerobic oxidation of methane, Nature, 407, 2000b, 623–626, doi:10.1038/35036572.

[9] Caldwell S.L., Laidler J.R., Brewer E.A., Eberly J.O., Sandborgh S.C., Colwell F.S., Anaerobic oxidation of methane: Mechanisms, bioenergetics, and the ecology of associated microorganisms, Environ Sci Technol. 42, 2008, 6791–6799.

[10] Crowe S.A., Katsev S., Leslie K., et al., The methane cycle in ferruginous Lake Matano, Geobiology 9(1), 2011, 61–78.

[11] Deutzmann J.S., Hoppert M., Schink B., Characterization and phylogeny of a novel methanotroph, *Methyloglobulus morosus* gen. nov., spec. nov. Sys. Appl. Microbiol. 37, 2014, 165–169, doi: 10.1016/j.syapm.2014.02.001.

[12] Deutzmann, J. S., Schink B., Anaerobic Oxidation of Methane in Sediments of Lake Constance, an Oligotrophic Freshwater Lake, Applied and Environmental Microbiology, 77, 2011, 4429–4436.
[13] Egger M., Jilbert T., Behrends T., Rivard C., Slomp C. P., Vivianite is a major sink for phosphorus in methanogenic coastal surface sediments, Geochimica et Cosmochimica Acta, 169, 2015, 217–235.
[14] Ettwig K.F., Butler M.K., Le Paslier D. et al., Nitrite-driven anaerobic methane oxidation by oxygenic bacteria, Nature 464(7288), 2010, 543–548.
[15] Ettwig K.F., Shima S., van de Pas-Schoonen K.T., Kahnt J., Medema M.H., op den Camp H.J.M., Jetten M.S.M., Strous M., Denitrifying bacteria anaerobically oxidize methane in the absence of Archaea, Environmental Microbiology, 10(11), 2008, 3164–3173, doi:10.1111/j.1462-2920.2008.01724.x.
[16] Ettwig K.F., van Alen T., van de Pas-Schoonen K.T., Jetten M.S.M., Strous M., Enrichment and molecular detection of denitrifying methanotrophic bacteria of the NC10 phylum, Appl. Environ. Microbiol., 75, 2009, 3656–3662.
[17] Ettwig K., Zhu B., Speth D., Keltjens J.T., Jetten M.S.M., Kartal B., Archaea catalyze iron-dependent anaerobic oxidation of methane, PNAS, 113, 45, 2016, 12792–12796, www.pnas.org/cgi/doi/10.1073/pnas.1609534113.
[18] Harder, J., Anaerobic methane oxidation by bacteria employing (super 14) C-methane uncontaminated with (super 14) C-carbon monoxide, In T. C. E. van Weering, G. T. Klaver, and R. A. Prins (ed.), Marine geology, Elsevier, Amsterdam, The Netherlands, vol. 137, 1997, 13–23.
[19] Haroon MF, et al., Anaerobic oxidation of methane coupled to nitrate reduction in a novel archaeal lineage, Nature 500(7464), 2013, 567–570.
[20] Hinrichs K.-U., Boetius A., The Anaerobic Oxidation of Methane: New Insights in Microbial Ecology and Biogeochemistry, Ocean Margin Systems, 2002, 457–477.
[21] Hinrichs K.-U., Hayes J.M., Sylva S.P., Brewer P.G., DeLong E.F., Methane-consuming archaebacteria in marine sediments, Nature, 398, 1999, 802–805.
[22] Hoehler T., M.J. Alperin, D.B. Albert, C.S. Martens, Field and laboratory studies of methane oxidation in an anoxic marine sediment: Evidence for a methanogen-sulfate reducer consortium, Global Biogeochemical Cycles 8(4), 1994, 451–463.
[23] Hu B., Shen L., Lian X., Zhu Q., Liu S., Huang Q., He Z., Geng S., Cheng D., Lou L., Xu X., Zheng P., He Y., Evidence for nitrite-dependent anaerobic methane oxidation as a previously overlooked microbial methane sink in wetlands, PNAS 111(22), 2014, 4495–4500.
[24] Intergovernmental Panel on Climate Change, Climate Change 2014, Mitigation of Climate Change, Summary for Policymakers and Technical Summary, 2015.
[25] Islas-Lima S., Thalasso, F., Gomez-Hernandez, J., Evidence of anoxic methane oxidation coupled to denitrification, Water Res., 38, 2004, 13–16.
[26] Iversen N., Jørgensen B.B., Anaerobic methane oxidation rates at the sulfate-methane transition in marine sediments from Kattegat and Skagerrak (Denmark), Limnology and Oceanography 30(5), 1985, 944–955, DOI: 10.4319/lo.1985.30.5.0944.
[27] Jones, R. I., Grey, J., Biogenic methane in freshwater food webs, Freshw. Biol. 56, 2011, 213–229. doi: 10.1111/j.1365-2427.2010.02494.x.
[28] Jones R.L.I., Whatley R.C., Cronin T.M., Dowsett H.J., Reconstructing late Quaternary deep-water masses in the eastern Arctic Ocean using benthonic ostracoda,

Marine Micropaleontology, 37(3–4), 1999, 251–272, https://doi.org/10.1016/S0377-8398(99)00022-5.
[29] Kankaala, P., Eller G., Jones R.I., Could bacterivorous zooplankton affect lake pelagic methanotrophic activity, Fundamental and Applied Limnology, 169, 2007a, 203–209.
[30] Kankaala P., Taipale S., Grey J., Sonninen E., Arvola L., Jones R.I., Experimental $\delta^{13}C$ evidence for a contribution of methane to pelagic food webs in lakes, Limnol. Oceanogr. 51(6), 2006, 2821–2827.
[31] Kankaala, P., Taipale S., Nykänen H., Jones R. I., Oxidation, efflux and isotopic fractionation of methane during autumnal turnover in a polyhumic, boreal lake, Journal of Geophysical Research–Biogeosciences, 112, 2007b, doi: 10.1029/2006JG000336.
[32] Knittel K., Boetius A., Anaerobic oxidation of methane: Progress with an unknown process. Annual Reviews of Microbiology, 63, 2009, 311–334.
[33] Knittel K., Lösekann T., Boetius A., Kort R., Amann R., Diversity and Distribution of Methanotrophic Archaea at Cold Seeps, Applied and Environmental Microbiology, 71(1), 2005, 467–479, https://doi.org/10.1128/AEM.71.1.467-479.2005.
[34] Lofton D., Whalen S. C., Hershey A. E., Effect of temperature on methane dynamics and evaluation of methane oxidation kinetics in shallow Arctic Alaskan lakes, Hydrobiologia 721(1), 2014, DOI: 10.1007/s10750-013-1663-x.
[35] Lösekann T., Knittel K., Nadalig T., Fuchs B., Niemann H., Boetius A. et al., Diversity and abundance of aerobic and anaerobic methane oxidizers at the Haakon Mosby mud volcano, Barents Sea, Appl. Environ. Microbiol., 73, 2007, 3348–3362.
[36] Maignien L., Parkes R.J., Cragg B., Niemann H., Knittel K., Coulon S., Akhmetzhanov A., Boon N., Anaerobic oxidation of methane in hypersaline cold seep sediments, FEMS Microbiol. Ecol, 83, 2013, 214–231.
[37] Martinez-Cruz K., Leewis M.-C., Herriott I. C., Sepulveda-Jauregui A., Anthony K. W., Thalasso F., Leigh M. B., Anaerobic oxidation of methane by aerobic methanotrophs in sub-Arctic, Science of the Total Environment, 607–608, 2017, 23–31.
[38] Milucka J., et al., Zero-valent sulphur is a key intermediate in marine methane oxidation. Nature, 491(7425), 2012, 541–546.
[39] Moran J.J., House C.H., Freeman K.H., Ferry J.G., Trace methane oxidation studied in several Euryarchaeota under diverse conditions, Archaea, 1, 2005, 303–309.
[40] Niemann H., Duarte J., Hensen C., Omoregie E., Magalhaes V.H., Elvert M., Pinheiro L.M., Kopf A., Boetius A., Microbial methane turnover at mud volcanoes of the Gulf of Cadiz, Geochimica et Cosmochimica Acta, 70, 2006, 5336–5355.
[41] Nordi K.A., Thamdrup B., Nitrate-dependent anaerobic methane´oxidation in a freshwater sediment, Geochim Cosmochim Acta, 132, 2014, 141–150.
[42] Nordi K., Thamdrup B., Schubert C. J., Anaerobic oxidation of methane in an iron-rich Danish freshwater Lake sediment, Limnol. Oceanogr., 58(2), 2013, 546–554, doi:10.4319/lo.2013.58.2.0546.
[43] Oni O., Miyatake T., Kasten S., Richter-Heitmann T., Fischer D., Wagenknecht L., et al., Distinct microbial populations are tightly linked to the profile of dissolved iron in the methanic sediments of the Helgoland mud area, North Sea. Front. Microbiol, 6(365), 2015, doi: 10.3389/fmicb.2015.00365.
[44] Pancost R.D., Sinninghe Damsté J.S., de Lint S., van der Maarel M.J., Gottschal J.C., Biomarker evidence for widespread anaerobic methane oxidation in Mediterranean sediments by a consortium of methanogenic archaea and bacteria, Applied and Environmental Microbiology, 66, 2000, 1126–1132.

[45] Raghoebarsing A.A., Pol A., van de Pas-Schoonen K.T., Smolders A.J., Ettwig K.F., Rijpstra W.I., Schouten S., Damsté J.S., Op den Camp H.J., Jetten M.S., Strous M., A microbial consortium couples anaerobic methane oxidation to denitrification, Nature, 440(7086), 2006, 918–921.
[46] Reeburgh, W., Oceanic methane biogeochemistry, Chem. Rev., 107, 2007, 486–513.
[47] Riedinger N., Formolo M. J., Lyons T. W., Henkel S., Beck A., Kasten S., An inorganic geochemical argument for coupled anaerobic oxidation of methane and iron reduction in marine sediments, Geobiology, 12(2), 2014, 172–181.
[48] Roland F. A. E., Morana C., Darchambeau F., Crowe S. A., Thamdrup B., Descy J.-P., Borges A. V., Anaerobic methane oxidation and aerobic methane production in an east African great lake (Lake Kivu), Journal of Great Lakes Research, 2018, (in press).
[49] Scheller S., Yu H., Chadwick G. L., McGlynn S. E., Orphan V. J., Artificial electron acceptors decouple archaeal methane oxidation from sulfate reduction, Science, 351(6274), 2016, 703–707, DOI: 10.1126/science.aad7154.
[50] Schlesinger W.H., Bernhardt E.S., Biogeochemistry: an analysis of global change, 2013.
[51] Schubert C. J., et al., Oxidation and emission of methane in a monomictic lake (Rotsee, Switzerland), Aquat. Sci., 72, 2010, 455–466, doi:10.1007/s00027-010-0148-5.
[52] Schubert C.J., Vazquez F., Lösekann-Behrens T., Knittel K., Tonolla M., Boetius A., Evidence for anaerobic oxidation of methane in sediments of a freshwater system (Lago di Cadagno), FEMS Microbiol Ecol., 76, 2011, 26–38.
[53] Sivan O., Adler M., Pearson A. et al., Geochemical evidence for ironmediated anaerobic oxidation of methane, Limnol Oceanogr., 56, 2011, 1536–1544.
[54] Smemo K.A., Yavitt J.B., Anaerobic oxidation of methane: an underappreciated aspect of methane cycling in peatland ecosystems?, Biogeosciences, 8, 2011, 779–793, https://doi.org/10.5194/bg-8-779-2011.
[55] Taipale, S., Kankaala P., Jones R. I., Contributions of different organic carbon sources to Daphnia in the pelagic food web of a small polyhumic lake: Results from mesocosm ^{13}C-additions, Ecosystems (N. Y., Print), 2008, doi:10.1007/s10021-007-9056-5.
[56] Thauer R.K., Shima S., Methane as fuel for anaerobic microorganisms, Ann N Y Acad Sci., 1125, 2008, 158–170.
[57] Timmers P.H., Suarez-Zuluaga D.A., van Rossem M. et al., Anaerobic oxidation of methane associated with sulfate reduction in a natural freshwater gas source, ISME J, 10, 2016, 1400–1412.
[58] Timmers P.H., Welte C.U., Koehorst J.J., et al., Reverse methanogenesis and respiration in methanotrophic Archaea, Archaea, 2017.
[59] Treude T., Knittel K., Blumenberg M., Seifert R., Boetius A., Subsurface microbial methanotrophic mats in the Black Sea, Appl. Environ. Microb., 71(10), 2005, 6375–6378.
[60] Trotsenko Y.A., Murrell J.C., Metabolic aspects of aerobic obligate methanotrophy, Advances in Applied Microbiology, 63, 2008, 183–229.
[61] Wankel S.D., Adams M.M., Johnston D.T., Hansel C.M., Joye S.B., Girguis P.R., Anaerobic methane oxidation in metalliferous hydrothermal sediments: influence on carbon flux and decoupling from sulfate reduction, Environ. Microbiol., 14, 2012, 2726–2740.

[62] Welte C.U., Nitrate- and nitrite-dependent anaerobic oxidation of methane, Environ. Microbiol. Rep., 8, 2016, 941–955.
[63] Zehnder A.J., Brock T.D., Methane formation and methane oxidation by methanogenic bacteria, J Bacteriol., 137(1), 1979, 420–432.

Przesłano do redakcji: 18.03.2019 r.

CZASOPISMO INŻYNIERII LĄDOWEJ, ŚRODOWISKA I ARCHITEKTURY
JOURNAL OF CIVIL ENGINEERING, ENVIRONMENT AND ARCHITECTURE
JCEEA, t. XXXVI, z. 66 (1/19), styczeń-marzec 2019, s. 27-35, DOI:10.7862/rb.2019.3

Adam PIECH[1]
Krzysztof TRZYNA[2]
Agata SKWARCZYNSKA-WOJSA[3]
Timothy DOUGLAS[4]

DISSOLVED ORGANIC CARBON AND BIODEGRADABLE DISSOLVED ORGANIC CARBON DETERMINATION IN RIVER WATER OF THE STRUG BASIN

The aim of the study was to determine Dissolved Organic Carbon (DOC) and Biodegradable Dissolved Organic Carbon (BDOC) concentrations, as well as the correlation between them, in the river water of the Strug basin located in the Carpathian Foothills. The Strug river's hydrographic basin was chosen for the study as it is a typical catchment area, which allows ease of measurement. DOC concentrations in the streams (tributaries) and the Strug ranged from 2.71 to 4.88 mgC/dm^3 and from 3.62 to 4.19 mgC/dm^3, respectively. BDOC concentrations in the streams and the Strug ranged from 0.40 to 1.09 mgC/dm^{3}and from 0.64 to 0.77 mgC/dm^3, respectively. BDOC, expressed as the percentage of DOC (%BDOC) ranged from 14.76 to 24.78% in the streams, and from 17.68 to 20.11% in the Strug. The procentage of BDOC is independent of DOC concentrations. The season of the year and the size of the watercourse had the greatest impact on DOC and BDOC concentrations.

Keywords: organic carbon, water quality, natural waters, water protection

[1] Adam Piech, Department of Civil, Environmental Engineering and Architecture, University of Technology, Powstancow Warszawy 6, 35-959, Rzeszow, Poland, https://orcid.org/0000-0002-7323-1155

[2] Krzysztof Trzyna

[3] Corresponding author: Agata Skwarczynska-Wojsa, Department of Civil, Environmental Engineering and Architecture, University of Technology, Powstancow Warszawy 6, 35-959, Rzeszow, Poland Rzeszow, https://orcid.org/0000-0003-3892-9176

[4] Timothy Douglas, Engineering Department, Gillow Avenue, Lancaster University, Bailrigg, LA1 4YW, United Kingdom, https://orcid.org/0000-0002-8069-8941

1. Introduction

Surface water in Poland is a significant source of water used for consumption and industrial purposes. Organic matter is its typical component, which is important from the point of view of water treatment processes [1]. Even though it does not have a direct impact on human health, organic matter decreases the efficiency of disinfectants and leads to the formation of harmful disinfection by-products [2,3]. Knowledge of the DOC biodegradable fraction content is also very important in the context of water stability in water distribution systems [4,5,6].

The major source of organic matter in temperate surface water is the terrestrial contribution [7]. The main factor affecting organic carbon concentration is net primary productivity, rather than direct biomass decomposition. It has been estimated that the fluvial export of organic matter from a given region is about 1% of the net primary productivity [8]. The content of clay minerals in catchment soils is also of great importance. In places where clay content is high, water contains less carbon [9] due to the sorption capacity of soils [10]. Atmospheric precipitation is also an important factor influencing DOC concentrations. It has been estimated that the mean concentration of organic carbon in rainwater is 1.932 mgC/dm^3. In warm seasons, DOC concentrations in continental precipitation were higher than in cold seasons [11]. Similar trends have been observed in analyses performed for areas near Rzeszow [12]. The median values recorded for spring, summer and autumn were 2.9, 2.8 and 1.83 mgC/dm^3, respectively.

Research carried out for over ten years has shown a gradual increase in DOC concentrations in surface water. In some regions of the UK, this content increased by an average of 91% in the years 1989–2004, and in the USA – by 10% in the years 1990–2000 [13]. The reason for this phenomenon is unknown. It is assumed that it is driven by climate change and the related cycles of excessive drying and moistening of soil, as well as changes in the soil sorption complex caused by continuous mineral acid inflow [14,15].

Although studies on the content of biodegradable fraction of DOC have been conducted for over a dozen years all over the world, so far no such research has been performed in Poland in the context of surface water.

The aim of the present study was to determine the concentration of DOC and determine the concentration of BDOC in the waters of the Strug River.

2. Materials and methods

2.1. Study area

The Strug basin is located on the border of two physical and geographical units:

1. Outer Carpathians (Flysch Carpathians)
2. Carpathian Foredeep

In terms of the hydrographic division, the area discussed is classified as the Upper Vistula water region, forming a combined water body marked with code GW0821, composed of two Surface Water Bodies (SWB). Table 1 presents basic information on the catchment area discussed.

Table 1. Register characteristics of the Strug river basin [16]

SWB code	SWB name	SWB type	SWB code	Catchment area [km^2]
RW2000122265689	"The Strug to the Chmielnicka river"	Flysch stream	12	238
RW2000142265699	"The Strug from the Chmielnicka river to the estuary"	Small flysch river	14	31.82

[Source: http://bip.rzeszow.rdos.gov.pl/files/artykuly/48023/Rejestr_JCWP.xls]

A part of the area discussed, located in the Carpathian Foredeep, filled with Tertiary formations and Miocene clays, lies at an elevation of 210-260 meters above sea level and is characterized by a small diversity of terrain. It is an area gently sloping towards the northwest, cut by the valleys of the Wislok river's tributaries.

Within the Wislok Valley, there are Pleistocene and Holocene river formations in the form of silty clays, sandy dusts and dusts, gravels and sands.

The Carpathian Foothills are built of low- and medium-resistant Carpathian flysch of the Skole unit with a layered structure. Deep valleys covered with Holocene river formations: sands, gravels and alluvial soils, were carved in the flysch formations. The Foothills consist of quite extensive plateaux and ridges at c. 300–460 meters above sea level. Relative elevation differences in this area reach up to 150 meters. Mass wasting occurs in the form of landslides and downhill creeps. The inclined areas, especially arable land, are prone to erosion. Locally, the valley bottoms are waterlogged.

A large part of the basin, i.e. approximately 90% of its area, is covered with saprolitic and slope soils of low permeability, such as clays and sands of varying thickness.

The average annual air temperature for the study area is 7.1–7.4°C, and the total annual precipitation amounts to 627–643 mm.

The sampling sites were located in the Ryjak, Chmielnik and Nieborow streams, and at the estuary of the Strug, upstream of where the river flows into the Rzeszow Reservoir. The sampling sites for stream water were located upstream of the sewage treatment plants. The site location is presented in Figure 1.

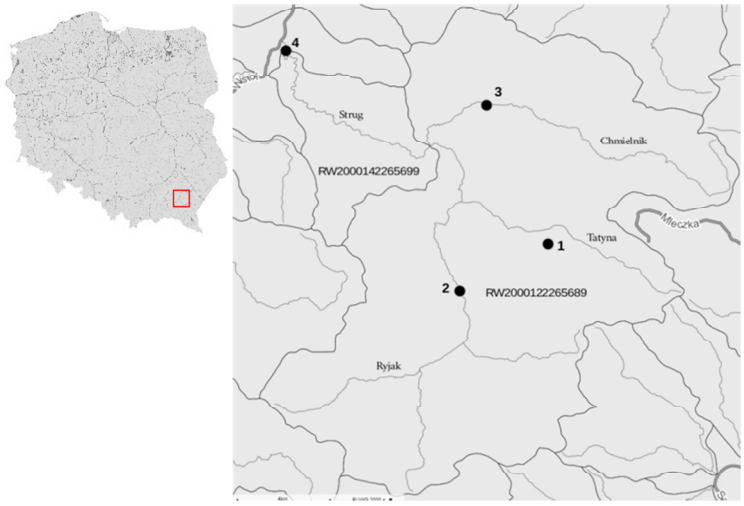

Figure 1. Sample collection sites within the Strug catchment area: 1–Nieborow stream, 2–Ryjak stream, 3–Chmielnik stream, 4–Strug River [Source: https://polska.e-mapa.net/]

2.2. BDOC and DOC determination methodology

Samples were collected quarterly with a Bürkle scoop with a telescopic rod adjusted to 500 ml bottles with a ground socket. Water samples were transported to the laboratory at refrigeration temperatures. The time between sample collection and the beginning of tests did not exceed 5 hours.

Servais' modified method for determination of BDOC in water was used in the analysis [17]. This method involves sterilizing the water sample by filtration, inoculating it with an autochthonous bacterial population, and incubating it for 28 days. The BDOC value is determined based on the difference between the DOC concentration before and after incubation.

$$BDOC = DOC_0 - DOC_i \quad (1)$$

where: BDOC – biodegradable dissolved organic carbon,
DOC_0 – dissolved organic carbon before incubation,
DOC_i – remaining dissolved organic carbon after incubation.

The analysis started with filtration of 200 ml of the sample analysed through a 0.2-µm-pore-size membrane filter (Whatman) which was first rinsed

with distilled water and then with the water sample. Two mililiters of inoculum containing autochthonous bacteria was added to the filtrate. The inoculum was a water sample filtered through a 0.2-µm-pore-size syringe filter (Whatman). This size of pores prevents the development of protozoa in the sample analysed.

The next stage of the analysis involved the determination of baseline DOC content in the sample (DOC_0). For that purpose, 40 ml of the water was collected and then analysed using a Sievers 5310 C TOC Analyser (GE) in accordance with the manufacturer's methodology. The remaining sample was incubated for 28 days in the dark, at 20°C, in a cone flask with a stopper allowing for gas exchange. After this time, DOC content was again determined in the sample (DOC_i).

The adopted method of BDOC analysis was verified with a test, which involved adding increasing doses of an organic carbon standard to water samples. These samples were a mixture of dechlorinated tap water and raw water from the Wislok river. The volume ratio was adjusted in such a way as to obtain a baseline DOC concentration of c. 0.5 mgC/dm^3. Increasing amounts of sodium acetate (source of easily biodegradable organic carbon) were added to the samples to increase DOC concentration (and, at the same time, BDOC concentration) by 0.5, 1.0 and 2.0 mgC/dm^3.

Before each use, the laboratory glassware was sterilised and cleaned to remove organic matter by heating for 4 h at 550°C in a muffle furnace. The steel filtration system was rinsed with a 10% solution of sodium persulfate at 50°C and then sterilised via autoclaving.

3. Results and discussion

The results of the method verification tests are presented in Table 2.

Table 2. Results of tests verifying the BDOC determination method

Day of incubation	**BDOC dose [mgC/dm^3]**			
	0	**0.50**	**1.00**	**2.00**
0	0.54	1.01	1.61	2.65
28	0.45	0.45	0.52	0.56
Difference	0.09	0.56	1.10	2.09

BDOC concentration in the water samples was 0.09 mgC/dm^3 i.e. 16.7% of the total DOC content. Data presented in Table 2 indicate that a corresponding increase of concentration was obtained for each BDOC dose after incubation. Importantly, the differences in DOC concentrations before and after incubation also reflect the BDOC fraction present in the test water.

The test results for DOC concentrations (average of two measurements) in the river water of the Strug catchment area are presented in Table 3.

Table 3. Seasonal variability in DOC

Season	DOC [mg/dm^3]			
	Nieborow stream	Ryjak stream	Chmielnik stream	Strug River
Spring (Sp)	2.71	3.20	3.38	3.62
Summer (Sm)	4.53	4.88	3.56	3.74
Autumn (A)	3.35	3.80	3.77	4.19
Winter (W)	2.78	3.06	2.93	3.78

The greatest seasonal variability in DOC concentrations was observed for water samples from the Nieborow and Ryjak streams – 1.82 mgC/dm^3. A slightly lower value was noted for the Chmielnik stream, and with the Strug, the seasonal variability was the lowest – 0.57 mgC/dm^3.

The season of the year influenced DOC concentrations in the waters analysed. The lowest concentrations in all sample collection sites were recorded in the winter and spring months. For the Nieborow stream and the Strug, the lowest concentrations were recorded in spring (2.71 and 3.62 mgC/dm^3, respectively). For the Ryjak and Chmielnik streams, on the other hand, the lowest values were observed in winter (3.06 and 2.93 mgC/dm^3, respectively).

Generally, DOC concentrations <3.0 mgC/dm^3 were found in 18.75% of the samples, 3.1-3.5 mgC/dm^3 in 25% of the samples, 3.5-4.0 mgC/dm^3 in 37.5% of the samples, and >4.0 mgC/dm^3 in 18.75% of the samples.

The results of BDOC concentration analysis for river water from the Strug catchment area are presented in Figure 2.

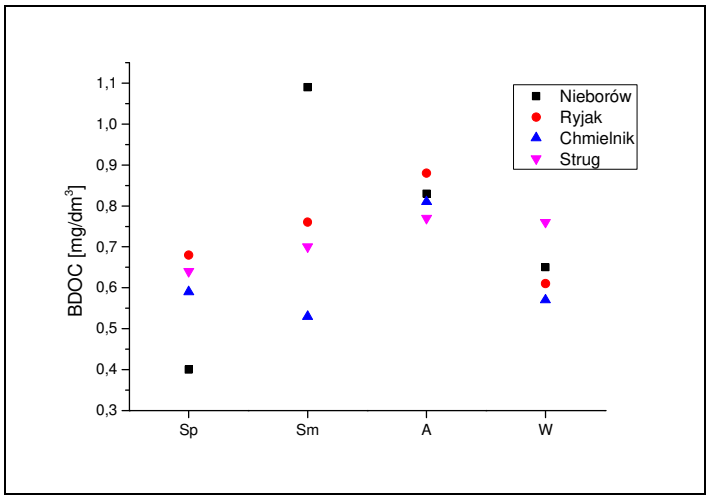

Figure 2. BDOC concentration [mgC/dm^3] Sp–spring, Sm–summer, A–autumn, W–winter

BDOC concentrations in the Strug basin streams ranged between 0.40 and 1.09 mgC/dm^3. Interestingly, these minimum and maximum values both pertained to the smallest flow i.e. the Nieborow stream. The range for the Strug was 0.64–0.77 mgC/dm^3. The %BDOC was 14.76–24.78% in the streams, and 17.68–20.11% in the Strug. As for seasonal changes, the lowest BDOC concentrations were recorded in spring and winter, and the highest – in autumn.

Figure 3 presents the general relation between DOC concentrations and BDOC expressed as the percentage of DOC. No correlation was found between these variables.

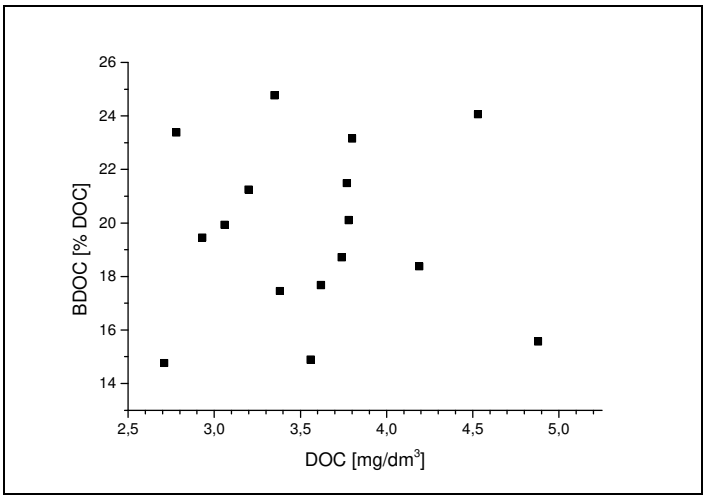

Figure 3. BDOC as the percentage of DOC in relation to DOC concentrations

DOC concentrations in flowing surface water change depending on the size of the watercourse, climate, type of the vegetation cover in the catchment area, and season of the year. The highest DOC concentrations of up to 50 mg mgC/dm^3 are found in watercourses beginning at marshes and peat-bogs [8]. In cool temperate climates, the typical range of DOC concentrations in rivers is 2–8 mgC/dm^3, with a mean of 3 mgC/dm^3. In their analysis, Servais et al. [17] demonstrated that DOC concentration in a river with a low level of pollution was c. 3.5 mgC/dm^3. Similar results were obtained in the present study. High variability in DOC concentrations has also been observed in catchment areas outside of Europe. In a study of the White Clay Creek watershed (North-eastern region of the USA), DOC concentrations ranged from 0.7 to 15.5 mgC/dm^3, with the peak %BDOC reaching 37.8% [18]. In the paper by Servais et al. [17], the BDOC fraction expressed as the percentage of DOC ranged between 19 to 34%. Similar results (20–25%) were obtained in the present study. A more extensive range has been observed for waters in areas closer to the North Pole. The %BDOC recorded by Fellman et al. [19] in three watersheds in Alaska ranged between 7 and 38%.

The present study demonstrated that DOC and BDOC concentrations varied depending on season. This was due to both accelerated organic matter decomposition at high temperatures and higher total precipitation in the summer and autumn months. DOC concentrations are also significantly affected by the size of watercourse – the smaller stream is, the greater the DOC concentration fluctuations. In the present study, this was observed in the Nieborow stream. The opposite was found for the estuary section of the Strug, where concentration fluctuations were the lowest.

4. Conclusions

1. DOC concentrations in the Strug and its tributaries (streams) ranged from 3.62 to 4.19 mgC/dm^3 and from 2.71 to 4.88 mgC/dm^3, respectively.
2. Seasons of the year and the size of the watercourse affect DOC concentrations in the river water of the Strug basin.
3. Except for the summer months, the greatest DOC concentrations were recorded at the sampling site located in the estuary section of the Strug.
4. The procentage of BDOC ranged between 14.76 and 24.78%.
5. In the Strug river basin, procentage of BDOC is independent of DOC concentrations.
6. Tests verifying the BDOC determination method proved its usefulness in analyses of natural waters.

References

[1] Sillanpää M. Natural Organic Matter in Water: Characterization and Treatment Methods. Butterworth-Heinemann; 2014.

[2] Świetlik J., Dąbrowska A., Raczyk-Stanisławiak U., Nawrocki J. Reactivity of natural organic matter fractions with chlorine dioxide and ozone. Water Res 2004;38:547–58. doi:10.1016/j.watres.2003.10.034.

[3] Villanueva CM., Cordier S., Font-Ribera L., Salas LA., Levallois P. Overview of Disinfection By-products and Associated Health Effects. Curr Environ Health Rep 2015;2:107–15. doi:10.1007/s40572-014-0032-x.

[4] Egli T. How to live at very low substrate concentration. Water Res 2010;44:4826–37. doi:10.1016/j.watres.2010.07.023.

[5] Wolska M. Biological stability of water in water distribution systems. The effect of water treatment trials. Environ Prot Eng 2015;41.

[6] Papciak D., Tchórzewska-Cieslak B., Pietrucha-Urbanik K., Pietrzyk A. Analysis of the biological stability of tap water on the basis of risk analysis and parameters limiting the secondary growth of microorganisms in water distribution systems. Desalination Water Treat 2018;117:1–8. doi:10.5004/dwt.2018.22106.

[7] Wilkinson GM., Pace ML., Cole JJ. Terrestrial dominance of organic matter in north temperate lakes. Glob Biogeochem Cycles 2013;27:43–51. doi:10.1029/2012GB004453.

[8] Thurman EM. Organic Geochemistry of Natural Waters. Springer; 1985.

[9] Nelson P., Cotsaris E., Oades J., Bursill D. Influence of soil clay content on dissolved organic matter in stream waters. Mar Freshw Res 1990;41:761–74.

[10] Nelson PN., Baldock JA., Oades JM. Concentration and composition of dissolved organic carbon in streams in relation to catchment soil properties. Biogeochemistry 1992;19:27–50. doi:10.1007/BF00000573.

[11] Willey JD., Kieber RJ., Eyman MS., Avery GB. Rainwater dissolved organic carbon: Concentrations and global flux. Glob Biogeochem Cycles 2000;14:139–148. doi:10.1029/1999GB900036.

[12] Zdeb M., Papciak D., Zamorska J. An assessment of the quality and use of rainwater as the basis for sustainable water management in suburban areas. E3S Web Conf 2018;45:00111. doi:10.1051/e3sconf/20184500111.

[13] Evans CD., Monteith DT., Cooper DM. Long-term increases in surface water dissolved organic carbon: Observations, possible causes and environmental impacts. Environ Pollut 2005;137:55–71. doi:10.1016/j.envpol.2004.12.031.

[14] Sarkkola S., Koivusalo H., Laurén A., Kortelainen P., Mattsson T., Palviainen M., et al. Trends in hydrometeorological conditions and stream water organic carbon in boreal forested catchments. Sci Total Environ 2009;408:92–101. doi:10.1016/j.scitotenv.2009.09.008.

[15] Hejzlar J., Dubrovský M., Buchtele J., Růžička M. The apparent and potential effects of climate change on the inferred concentration of dissolved organic matter in a temperate stream (the Malše River., South Bohemia). Sci Total Environ 2003;310:143–52. doi:10.1016/S0048-9697(02)00634-4.

[16] Rozporządzenie Ministra Środowiska z dnia 22 lipca 2009 r. w sprawie klasyfikacji stanu ekologicznego, potencjału ekologicznego i stanu chemicznego jednolitych części wód powierzchniowych Dz.U. z 2009 r. nr 122, poz. 1018

[17] Servais P., Anzil A., Ventresque C. Simple method for determination of biodegradable dissolved organic carbon in water. Appl Environ Microbiol 1989;55:2732–2734.

[18] McLaughlin C., Kaplan L.A. Biological lability of dissolved organic carbon in stream water and contributing terrestrial sources. Freshw Sci 2013;32:1219–30. doi:10.1899/12-202.1.

[19] Fellman J.B., Hood E., D'Amore D.V., Edwards R.T., White D. Seasonal changes in the chemical quality and biodegradability of dissolved organic matter exported from soils to streams in coastal temperate rainforest watersheds. Biogeochemistry 2009;95:277–93. doi:10.1007/s10533-009-9336-6.

Przesłano do redakcji: 10.02.2019 r.

CZASOPISMO INŻYNIERII LĄDOWEJ, ŚRODOWISKA I ARCHITEKTURY
JOURNAL OF CIVIL ENGINEERING, ENVIRONMENT AND ARCHITECTURE
JCEEA, t. XXXVI, z. 66 (1/19), styczeń-marzec 2019, s. 37-44, DOI:10.7862/rb.2019.4

Daniel TOKARSKI[1]
Wioletta ŻUKIEWICZ-SOBCZAK[2]
Marta CHODYKA[3]
Tomasz GRUDNIEWSKI[4]
Jerzy Antoni NITYCHORUK[5]
Robert TOMASZEWSKI[6]

COMPUTER SIMULATION OF HEATING PROPERTIES IN WALL PARTITION WITH BUILT-IN ELEMENTS THAT IMITATE THERMAL BRIDGES

The article aimed at presenting of the design assumptions of the wall partition built anda results of computer simulation of thermal properties in a heterogeneous wall partition in THERM. Display of the isotherms' distribution, heat flux vectors and temperature distribution in the area of thermal bridges and beyond. The tested partition on the basis of which simulations were created, was equipped with elements imitating thermal bridges, used in construction, to show their influence on the thermal properties of building structures. Thermal bridges can take the form of linear and point bridges. The example described in the article concerns the problem of thermal bridges occurring in wall partitions. The simulation is a preliminary pilot action before the start of non-invasive tests, ie measurement and calculation of the heat transfer coefficient, thermovision measurements on the surface of the barrier.

Keywords: 2D modeling, thermal permeability, thermal flows, point and linear thermal bridges

[1] Corresponding author: Daniel Tokarski, Państwowa Szkoła Wyższa im. Papieża Jana Pawła II w Białej Podlaskiej, Wydział Nauk Ekonomicznych i Technicznych, ul. Sidorska 95/97, 21-500 Biała Podlaska; tel. 833446921; d.tokarski@pswbp.pl
[2] Wioletta Żukiewicz-Sobczak, Państwowa Szkoła Wyższa im. Papieża Jana Pawła II w Białej Podlaskiej, Wydział Nauk Ekonomicznych i Technicznych, ul. Sidorska 95/97, 21-500 Biała Podlaska; wiola.zukiewiczsobczak@gmail.com
[3] Marta Chodyka, Państwowa Szkoła Wyższa im. Papieża Jana Pawła II w Białej Podlaskiej, Wydział Nauk Ekonomicznych i Technicznych, ul. Sidorska 95/97, 21-500 Biała Podlaska; m.chodyka@dydaktyka.pswbp.pl
[4] Tomasz Grudniewski, Państwowa Szkoła Wyższa im. Papieża Jana Pawła II w Białej Podlaskiej, Wydział Nauk Ekonomicznych i Technicznych, ul. Sidorska 95/97, 21-500 Biała Podlaska; gisbourne2@gmail.com
[5] Jerzy Antoni Nitychoruk, Państwowa Szkoła Wyższa im. Papieża Jana Pawła II w Białej Podlaskiej, Wydział Nauk Ekonomicznych i Technicznych, ul. Sidorska 95/97, 21-500 Biała Podlaska; wnet.dziekan@pswbp.pl
[6] Robert Tomaszewski, Państwowa Szkoła Wyższa im. Papieża Jana Pawła II w Białej Podlaskiej, Wydział Nauk Ekonomicznych i Technicznych, ul. Sidorska 95/97, 21-500 Biała Podlaska; r.tomaszewski@dydaktyka.pswbp.pl

1. Introduction

Computer simulation is a simulation using a mathematical model, saved in the form of a computer program. Simulation techniques are particularly useful where the analytical determination of the solution would be too labor-intensive, and sometimes even impossible, which often takes place in complex systems.

There is now one program available in Polish on the Polish market - SAT supporting the calculation of two-dimensional elements in accordance with the norm 10211: 2008 [8]. The program is quite complicated to use, especially for less-competent computer engineers. On the Internet you can find a lot of computing tools available commercially or free of charge, including eg DAVID 32, HAM-lab, Unorm, Champs-bes, or the THERM program. Programs dedicated to construction are primarily a classic electronic catalog of heat bridges "EUROKOBRA" [3]. The "Unorm" version 2012 and "David 32" are an intermediate version between the catalog and the calculation program. The programs do not give the designer full possibilities of independent modeling of any architectural detail, but they will be useful in engineering practice for typical solutions used mainly in frame building.

THERM is a computer program operating in the Microsoft Windows operating system. Developed at the Lavrence Berkeley National Laboratory, designed for architects, construction engineers, academic teachers, students of building departments, architecture, and other people interested in heat exchange problems in architectural details. Using the THERM 7.4 program. it is possible to model two-dimensional heat flow in building details such as: windows, walls, roofs, foundations and others in which thermal bridges are a significant problem. Analyzes made using THERM allow correct calculation of the heat flux density and temperature field in the cross-section. Two-dimensional heat flow calculations are based on the finite element method (FEM) [1], which enables modeling of geometrically complex architectural and building sections with 1 mm accuracy.

Completed calculations for practically any detail while maintaining the requirements as to its geometry as in the standard [9], allows to determine partial (edge) heat transfer coefficients UX and UY, and consequently to determine the linear heat transfer coefficient [W/mK]. Determining the temperature at any point of the nodes of the two-dimensional element, including anywhere on the inner edge, allows you to calculate the temperature factor fRsi, which is required in the construction project. The graphical interface allows you to plot cross-sections of the analyzed elements with known dimensions or import ready-made drawings in the form of dxf files. or bmp graphic files.

The results of calculations are obtained in the form of: 1) graphic, including: - isothermal distribution in the cross-section of the modeled element, - a colored temperature field in the cross-section, - a colored heat flux density

field. 2) textual, including: - heat transfer coefficients U [W/(m^{2}K)], - heat flux value [W/m], - flux density [W/m^2]. Obtained results in the form of colored drawings can be easily transferred to any graphic program or text editor. Additionally, you can generate a MES grid with node numbering [2].

The example described in the article concerns the problem of thermal bridges occurring in wall partitions. Unfortunately, thermal bridges can not be removed, but only reduce their impact. The negative effects of thermal bridges, apart from the increased loss of heat, are also the lowering of temperature on the surface of the existing bridge, condensation of water vapor, excessive settling of the dust and the possibility of mold fungi. The bridge is usually created by the presence of materials in these places, which have a higher thermal conductivity coefficient λ [W/(m·K)] than the remaining part of the barrier [5,7].

The existence of thermal bridges are easy to locate using the thermal image of the external and internal walls of the building. Bridges increase energy losses because the local temperature value in certain areas of the building envelope is greater. In this place, the heat escapes into the environment due to the increase in temperature, which causes an increase in radiation and convective flow [4].

2. Methodology of the research

The study was conducted in two similarly constructed rooms and the laboratory which was established in the premises of the Student Dormitory in the PSW in Biala Podlaska.

To install the research partition, the laboratory room was divided into two parts, i.e. the transmitting and receiving rooms (figure 1). The transmitting room was heated while the receiving one was cooled to obtain the highest possible temperature difference on both sides of the partition [6]. Next, thermal bridges were located in the partition in the form of elements of different heat transfer coefficient (linear and point) distributed as shown in the figure 2 and 3.

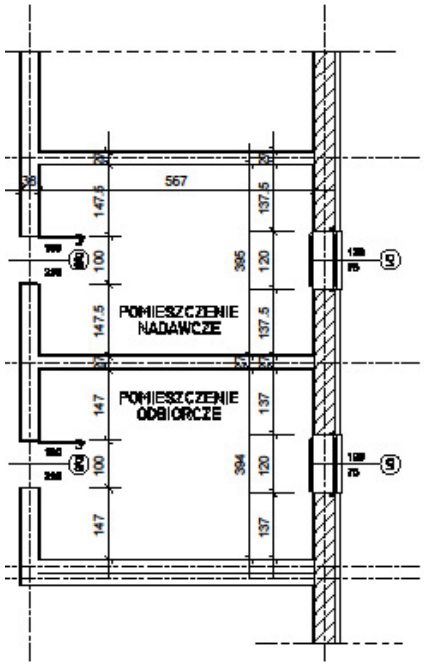

Fig. 1. Projection of rooms

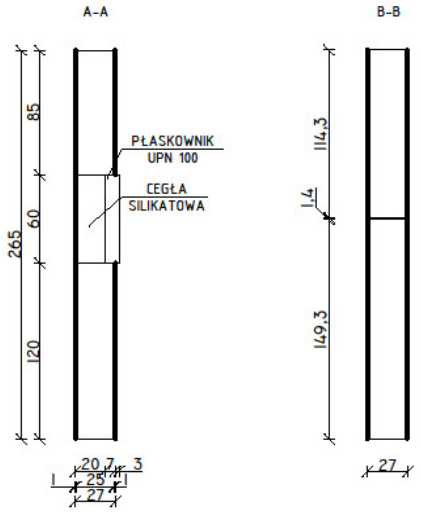

Fig. 2. Sections in the partition

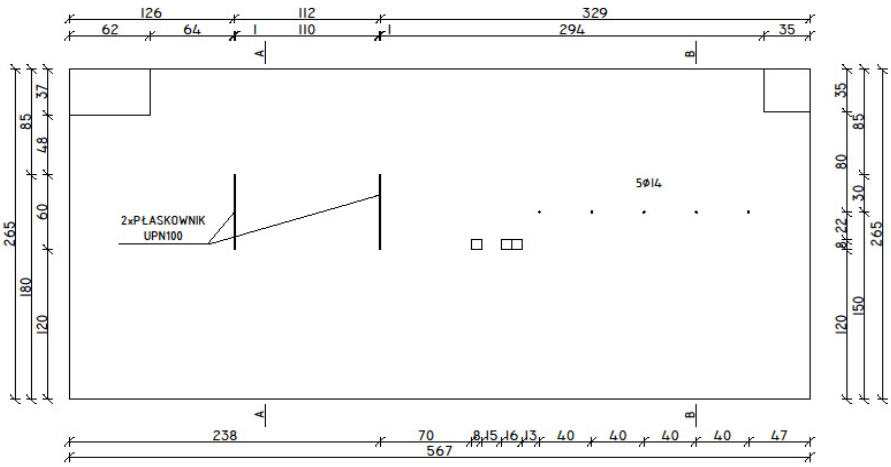

Fig. 3. View of the partition from the reception room

To make the bridges, the following elements were used: 2 UPN 100 flat bars (heat transfer coefficient λ = 58,00 W/(m·K); weight 10,6 kg/m), steel bars 5 x Φ 14 mm (coefficient of thermal conductivity λ = 58,00 W/(m·K); each 30 cm long), gypsum internal plaster (thermal conductivity coefficient λ = 0,40 W/(m·K);

density ρ = 1000 kg/m^3). Five drillings of Φ 14 mm were made, in which steel rods were located. The next step was to cut out furrows with an angle grinder measuring 10 × 60 cm into the two UPN 100 flat bars. Before placing the linear bridges in the proper place, the holes were adapted to the dimensions of the flat bar by forging.

3. Computer simulation of the thermal properties of the partition

THERM has created a simulation of an exemplary homogeneous partition model with vertical and horizontal cross-sections running through the partition with the following boundary conditions:

- External: temperature 6.3°C, heat transfer coefficient λ= 9 W/(K·m^2),
- Internal: temperature 23°C, heat transfer coefficient λ= 29,7 W/(K·m^2).

Selected architectural details have been adopted for calculations the following material data and characterizing them heat conduction coefficients:

- UPN 100 flat bars, heat transfer coefficient λ= 58,00 W/(m·K),
- Steel bars Φ 14 mm, coefficient of thermal conductivity λ=58,00 W/(m·K),
- Gypsum internal plaster, thermal conductivity coefficient λ= 0,40 W/(m·K).

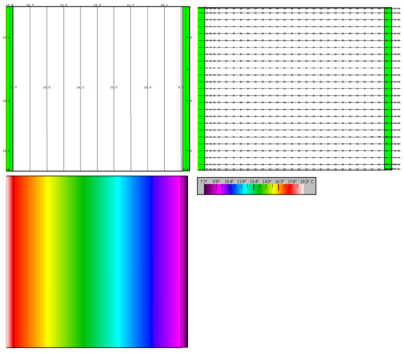

Fig. 4. Homogeneous partition as a case study of isothermal distribution, heat flow vectors and temperature distribution

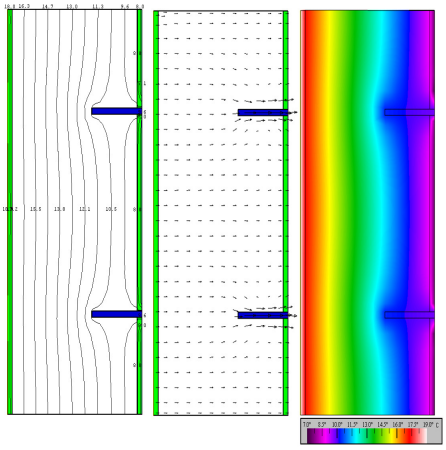

Fig. 5. Isothermal distribution, heat flux vectors and temperature distribution in the area of the partial linear bridge – a horizontal cross-section

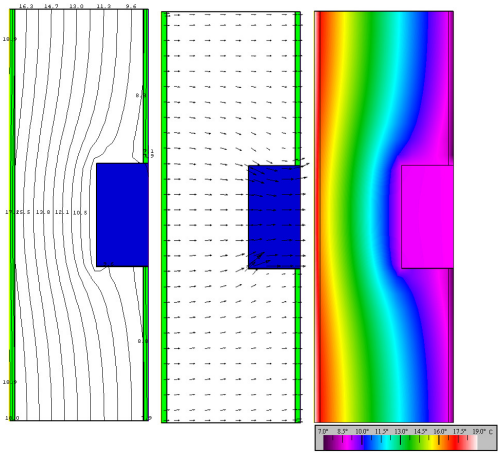

Fig. 6. Isothermal distribution, heat flux vectors and temperature distribution in the area of a partial linear bridge – vertical cross-section

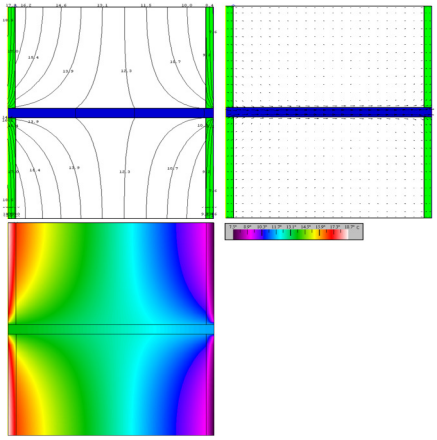

Fig. 7. Isothermal distribution, heat flux vectors and temperature distribution in the area of point bridge – a horizontal cross-section

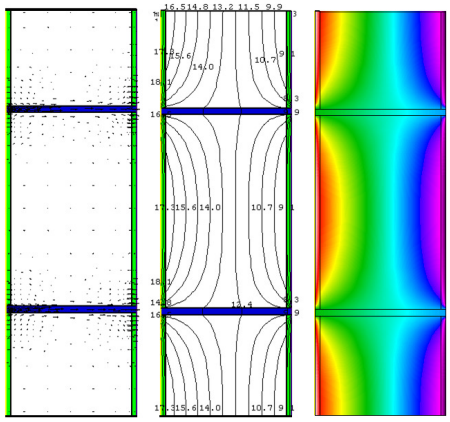

Fig. 8. Section of the baffle in the place where point bridges are located – horizontal cross-section (vectors of heat intensity, isothermal distribution, temperature distribution)

4. Conclusions

The presented results of a computer simulation of a building partition which was designed in accordance with the information provided by construction and thermal physics data, which is supposed to allow for explaining some selected problems, showed a clear negative effect of the built-in thermal bridges on the thermal properties of the partition.

In the case of the homogeneous partition, the isotherms are parallel, and the vectors of the heat flux intensity are perpendicular to the surface of the baffle, which is in line with the theory of heat flow (figure 4).

In the case of the area in which the partial linear heat bridges are located, the isotherms cease to be parallel to the surface of the partition. Then, two-way heat flow is visible, as indicated by the heat flow vectors. The vectors are no longer perpendicular to the surface of the baffle in the area of the linear bridge, which means that the heat flows not only from one surface to the other but in this case also vertically (figure 5,6).

In the case of the area in which point thermal bridges are located, the isotherms cease to be parallel to the surface of the partition. Then, two-way heat flow is visible, as indicated by the heat flow vectors. The vectors are no longer perpendicular to the surface of the baffle in the area of the point bridge, which means that the heat flows not only from one surface to the other, but also, as in this case, vertically (figure 7,8).

The building divider was designed based on the information collected in the field of construction and thermal physics, so that it is possible to explain selected issues in a simple way. To sum up, in order that the bulkhead can be used as a teaching aid in laboratory exercises in thermal physics of buildings, rooms should be adequately cooled or heated in order to increase the temperature difference around 15–20°C.

The simulation is a preliminary pilot action before the start of non-invasive tests, ie measurement and calculation of the heat transfer coefficient, thermovision measurements on the surface of the barrier. The results thermographic analysis wall partition with built-in elements that imitate thermal bridges are presented in the next article in the series.

References

[1] Gawin D., Komputerowa Fizyka Budowli, komputerowa symulacja procesów wymiany masy i energii w budynkach, KFBiMB, Łódź 1998.

[2] Grabarczyk S., Komputerowe wspomaganie projektowania budownictwa energo-oszczędnego, Oficyna Wydawnicza Politechniki Warszawskiej, Warszawa 2005.

[3] Heim D., Błaszczyk E., Ocena możliwości wykorzystania energii odnawialnej w oparciu o analizy statystyczne i symulacje komputerowe, Budownictwo

i inżynieria środowiska, Zeszyty Naukowe Politechniki Rzeszowskiej, nr 252 z. 47, Rzeszów 2008.

[4] Kisilewicz T., Królak E., Pieniążek Z., Fizyka cieplna budowli, Wydawnictwo Politechniki Krakowskiej, Kraków 1998.

[5] Klemm P., Budownictwo ogólne, tom 2, Fizyka budowli, Wydawnictwo Arkady, Warszawa 2006.

[6] Krause P., Steidl T., Orlik-Kożdoń B. Cieplnowilgotnościowe projektowanie ścian z betonu komórkowego. Zeszyt 3 Część 2 Mostki termiczne. SPB. Warszawa 2016.

[7] Norma, PN-EN ISO 10211-1: 1998 Mostki cieplne w budynkach. Strumień cieplny i temperatura powierzchni. Ogólne metody obliczania.

[8] PN-EN ISO 10211:2008, Mostki cieplne w budynkach. Strumienie ciepła i temperatury powierzchni. Obliczenia szczegółowe.

[9] PN-EN ISO 14683:2008, Mostki cieplne w budynkach, Liniowy współczynnik przenikania ciepła, Metody uproszczone i wartości orientacyjne.

Przesłano do redakcji: 20.07.2018 r.

CZASOPISMO INŻYNIERII LĄDOWEJ, ŚRODOWISKA I ARCHITEKTURY
JOURNAL OF CIVIL ENGINEERING, ENVIRONMENT AND ARCHITECTURE
JCEEA, t. XXXVI, z. 66 (1/19), styczeń-marzec 2019, s. 45-55, DOI:10.7862/rb.2019.5

Paweł KUT[1]

THE IMPACT OF WIND FARMS ON ACTIVE POWER LOSSES IN THE POWER SYSTEM

Increasing emission standards and European Union policy require investment in the renewable energy sector. An increasing amount of renewable energy sources, including wind farms, requires changes in the power system in countries whose energy is based on large system power plants, mostly coal-fired. Stricter share of renewable energy sources in energy mix, may improve the country's security and ensure the diversification of fuels and the gradual independence of conventional fuels. Thanks to regulation possibilities of doubly-fed induction generators, which are equipped with a significant part of wind turbines, it is possible to obtain better electricity parameters. The location of energy sources near the receiving nodes has a positive effect on the active power losses in the power system. This article analyzes the impact of a 30 MW wind farm on the level of active power losses in the power system, taking into account the different power factor values with which the wind farm can work. Simulation were carried out using the Powerworld Simulation software.

Keywords: wind farm, power system, active power losses

1. Introduction

The development of civilization is the cause of the growing demand for electricity [1]. The prospect of depletion of natural energy sources such as coal, gas and oil makes it necessary to search for new energy sources and increase the share of alternative energy sources based on renewable resources. As a result, renewable energy sources account for an increasing share of electricity production [2]. According to data prepared by the Polish National Energy Conservation Agency, electricity consumption in Poland will increase from 165.8 TWh in 2017 to nearly 230 TWh by 2040 [3]. According to this report, the share of renewable energy sources will increase to about 33%, the share of coal will fall to 33%, while the remaining 34% will go to nuclear, natural gas and lignite.

Wind and photovoltaic power plants are among the most popular sources of electricity coming from renewable sources in Poland. According to data from the Polish Energy Regulatory Office [4], in 2018 the total installed capacity in wind

[1] Paweł Kut, Politechnika Rzeszowska, Zakład Ciepłownictwa i Klimatyzacji, al. Powstańców Warszawy 6, 35-959 Rzeszów; tel. 178651147; p.kut@prz.edu.pl. https://orcid.org/0000-0002-2472-0454

power plants amounted to 5 874.778 MW, which accounted for 68.43% of the installed capacity in renewable energy sources in Poland.

A large number of wind farms connected to the power system has an impact on the level of active power losses in the power system [5]. The paper presents the analysis of active power losses in a given fragment of the power system depending on the reactive power generated, to which a wind farm consisting 10 wind turbines has been connected. Simulation were carried out using the Powerworld Simulator, which enables to analysis of the active and reactive power distribution.

2. Active power losses in transmission lines

Active power losses are associated with any process of generation, transmission and use of electricity [6,7]. Active power losses in the power system can be divided into load losses, which depend on the load and no-load losses, which in practice don't depend on the load. The general formula for active power losses can be represented by equation:

$$P = \int_V J^2 \rho dV \tag{1}$$

where: J – current density, ρ - conductive material resistivity, V – volume of the conductive element.

In the case of a homogenous track of which the cross-section is constant:

$$P = I^2 R \tag{2}$$

where: I – current, R – resistance.

The active power losses associated with transmission line load can be calculated using the equation [8]:

$$\Delta P_L = 3I^2 R = 3\left(\frac{S}{\sqrt{3}U}\right)^2 R = \frac{S^2}{U^2} R = \frac{P^2 + Q^2}{U^2} R \tag{3}$$

where: S – apparent power, Q – reactive power, U – phase to phase voltage.

No-load losses of active power shall be determined for network element in which the substitution schemes take into account the conductance. No-load losses can be calculated using the equation:

$$\Delta P_j = U^2 G \tag{4}$$

where: G – conductance of the network element.

Resultant active power losses can be determined by the equation:

$$\Delta P = \Delta P_L + \Delta P_j \tag{5}$$

3. Analysis of active power losses in the power grid

Simulations of active power losses were carried out for a wind farm consisting of 10 Vestas V90 - 3 MW wind turbines (WT1-WT10). Figure 1 shows the relation between active and reactive power of the analyzed wind turbines with doubly-fed induction generators [9,10, 11]. The 30 MW wind farm was connected to the 110 kV power system. The designed wind farm will have a radial structure. The wind farm consists of three radial lines connected to the main power supply point located on the area of the wind farm. In the case of a radial structure, damage to the cable stops the transmission of energy from the wind turbines located behind the damaged part of the internal grid. Greater reliability is characterized by a loop system, which in the event of a cable failure does not cause the power plant to shut down. It should be noted that the internal network of the wind farm is much more reliable than the wind turbines themselves, so in the case of a wind farm consisting of 10 wind turbines, it is more cost-effective to use the radial structure.

The diagram of the internal grid of the wind farm is presented in Figure 2.

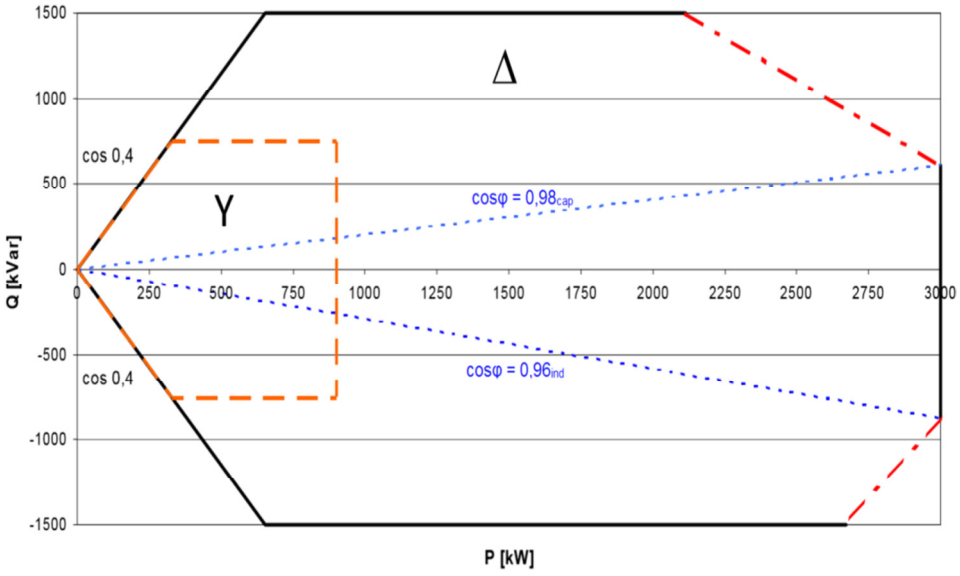

Fig. 1. Characteristic of the Vestas V90 – 3 MW wind turine [12]

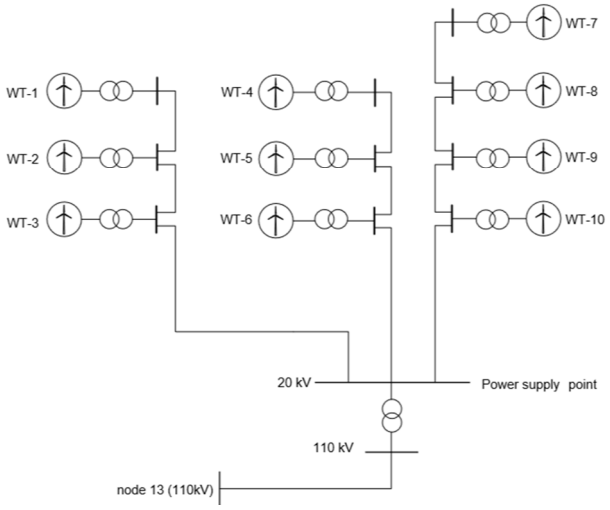

Fig. 2. Wind farm internal network

Figure 3 shows a 110 kV power system model made in Powerworld Simulator software. Wind farm was connected to node 13.

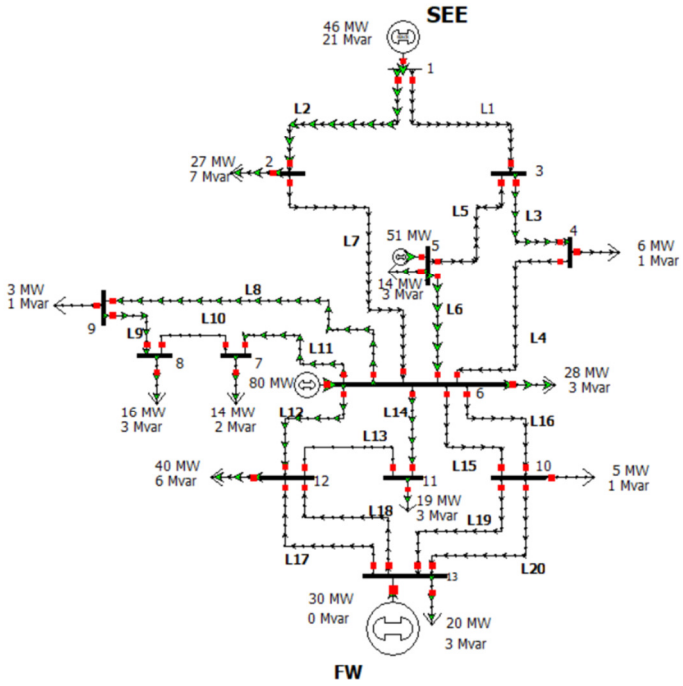

Fig. 3. Power system to which the wind farm is connected

Table 1 shows the transmission lines lengths and used cables and table 2 shows the exact values of active and reactive power received at the nodes.

Table 1. Line lengths and used cables

Line	Conductor	Lenght [km]	Line	Conductor	Lenght [km]
L1	240 AlFe	6.980	L11	240 AlFe	24.452
L2	240 AlFe	8.200	L12	185 AlFe	33.223
L3	185 AlFe	6.000	L13	185 AlFe	24.775
L4	185 AlFe	33.297	L14	185 AlFe	29.333
L5	185 AlFe	13.031	L15	450 AlFe	53.793
L6	185 AlFe	22.329	L16	450 AlFe	53.834
L7	150 AlFe	28.158	L17	185 AlFe	29.164
L8	240 AlFe	22.272	L18	185 AlFe	29.168
L9	240 AlFe	9.096	L19	240 AlFe	9.674
L10	240 AlFe	50.050	L20	240 AlFe	9.681

Table 2. Received active and reactive power

Node number	P [MW]	Q [MVar]	Node number	P [MW]	Q [MW]
1	-	-	8	15.7	3.4
2	27	6.8	9	3.0	1.0
3	-	-	10	4.5	1.1
4	5.6	1.4	11	19.0	3.4
5	14.5	3.4	12	35.8	5.6
6	28.0	3.4	13	15.7	2.2
7	14.5	2.2	-	-	-

The simulations were carried out for different values of active and reactive power generated by the wind farm. The output values of active and reactive power at the connection point of the wind farm were calculated on the basis of simulation of the wind farm's internal network. Internal network model was also made in Powerworld Simulator. Simulations of the internal network were carried out for all anylazed cases in order to determine the output parameters of wind warm taking into account the active power losses in the wind farm network. Active and reactive power generated by individual wind power plants was determined on the basis of the characteristics of Vestas V90. Simulations were made for power factors for which the wind farm works with maximum production of active power - $cos\varphi = 0.98_{cap}$, $cos\varphi = 0.96_{ind}$ and for power factors for which the farm works with undervalued active power which enables higher generation of reactive power.

Figure 4 shows the losses of active power in 110 kV lines in the case of wind turbines operating at a wind speed of 5 m/s. The output power of the entire wind farm is about 1.76 MW.

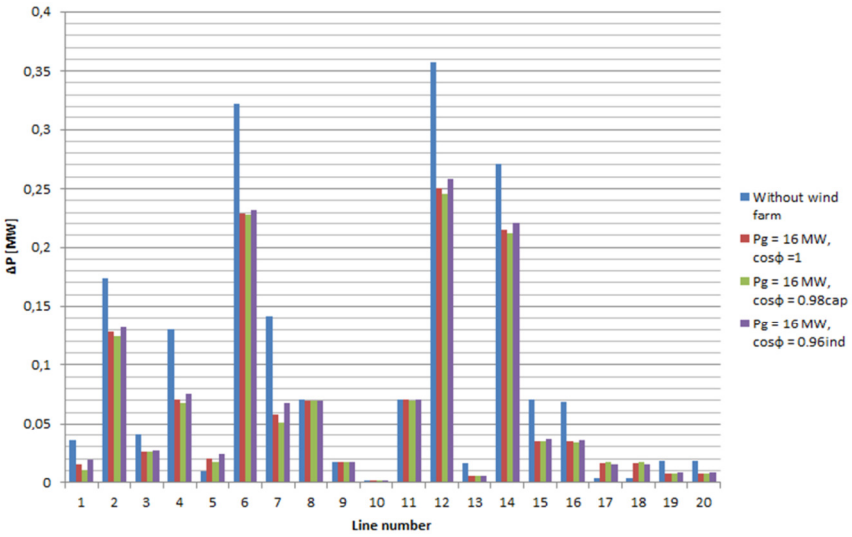

Fig. 4. Active power losses at wind speed of 5 m/s

It can be seen that active power losses in the power system after connection of the wind farm are reduced in comparison to the losses before connection. At low value of generated active power P_g the losses of active power in transmission lines are similar for the analyzed values of power factor $cos\varphi$.

Figure 5 shows losses of active power in the grid after connecting a wind farm with the generated power at the wind speed of 10 m/s. The output active power generated by entire wind farm is about 16 MW.

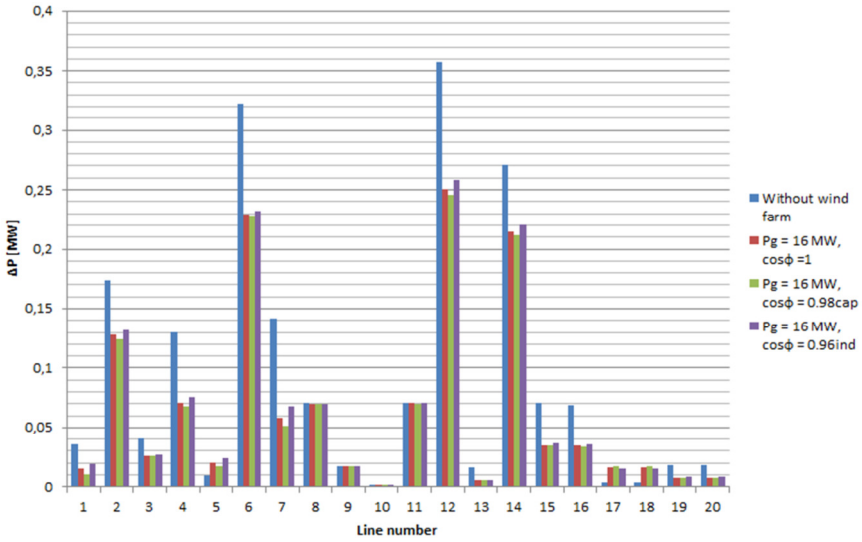

Fig. 5. Active power losses at wind speed of 10 m/s

Active power losses in lines L17 and L18 increases due to the higher current flow in the transmission lines, which is caused by a higher generation of active power, but the overall power losses in the network decreases significantly. When a wind farm consume reactive power from power system, the active power losses are higher than for a wind farm that delivers reactive power to the grid. Losses of active power in the case of a wind farm operating with power factor $cos\varphi = 0.98_{cap}$ are smaller in comparison to the operation with the power factor $cos\varphi = 1$ and for $cos\varphi = 0.96_{ind}$ higher.

Figure 6 shows the active power losses for a wind farm operating with rated power.

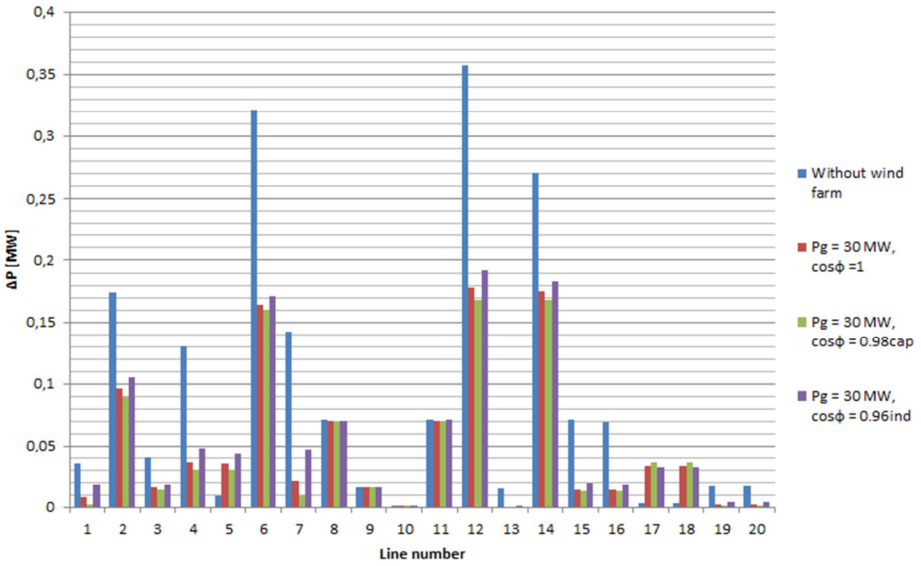

Fig. 6. Active power losses with rated power

Power losses in lines L17 and L18 increase, but total power losses decreased significantly, while in L6 and L12 lines active power losses are 50% lower in relation to grid operation without a wind farm.

Figure 7 shows the losses in case of a wind farm operating with $cos\varphi_{cap}$ and undervalued active power with maximum reactive power generation. The simulations were carried out for wind turbines operating with power:

- P_g = 0.8 MW, Q_g = 750 kVar;
- P_g = 2.0 MW, Q_g = 1500 kVar.

Due to operation with undervalued active power it is possible to achieve a higher voltage at the connection point and in nearby nodes. This allows the wind farms to be used for voltage regulation process.

Higher losses of active power in comparison to a wind farm operating with a power factor $cos\varphi = 0.98_{cap}$ are associated with a much smaller generation of active power.

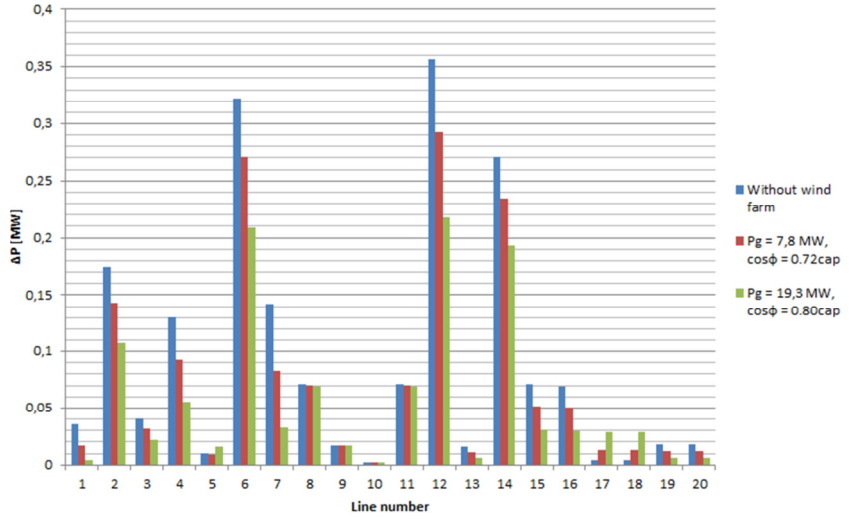

Fig. 7. Active power losses with undervalued active power and $cos\varphi_{cap}$

Figure 8 shows active power losses when the farm is working with $cos\varphi_{ind}$ with undervalued active power. Simulations were carried out for wind turbines operating with:

- P_g = 0.8 MW, Q_c = 750 kVar;
- P_g = 2.5 MW, Q_c = 1500 kVar.

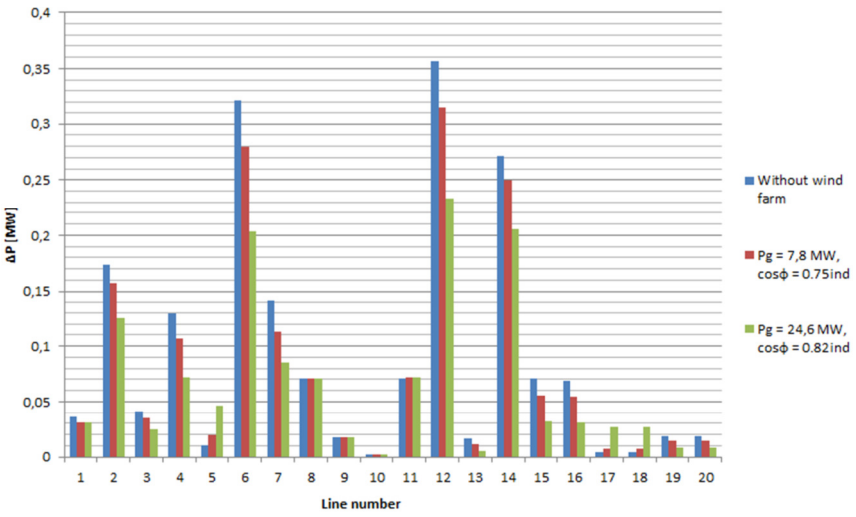

Fig. 8. Active power losses with undervalued active power and $cos\varphi_{ind}$

In that case wind farm consume reactive power from the grid. Consumption of reactive power from the grid may reduce the voltage at the connection point.

It is also possible to maintain a constant voltage when the generated active power increases. As the wind farm becomes another reactive power receiver in the power system, the reactive power line load increases and consequently the active power losses in the grid increases in relation to $cos\varphi_{poj}$.

Figure 9 shows the total active power losses in all transmission lines in the analyzed part of the power system.

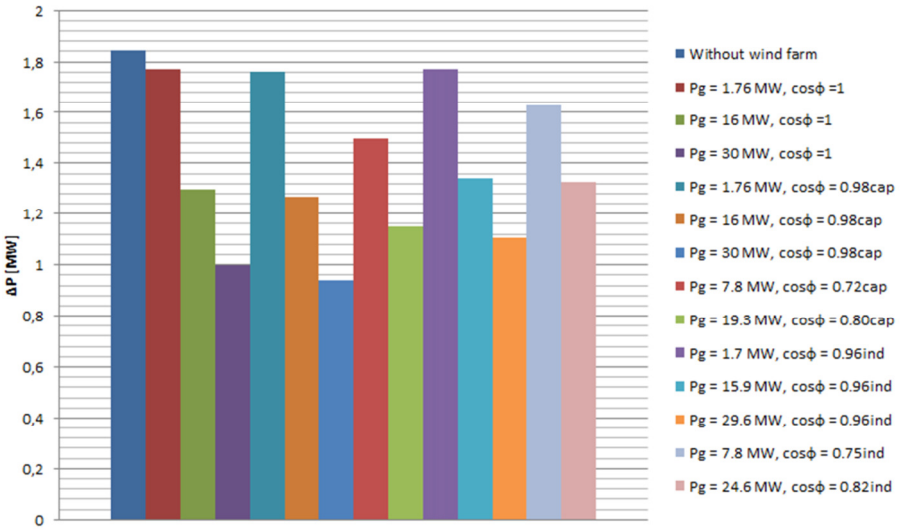

Fig. 9. Total active power losses in analysed grid

On the basis of the above graph it appears that the smallest active power losses in analyzed network occur during the operation of a wind farm with rated active power generation and power factor $cos\varphi = 0.98_{cap}$.

4. Conclusion

Decentralized energy production offers greater opportunities for efficient energy distribution. A larger share of distributed energy sources using renewable energy sources makes it possible to reduce dependence on fossil fuels and increases the security of the power system based on large system power plants.

By connecting generation sources nearby consumers, active power losses in transmission lines can be significantly reduced. The generation of reactive power nearby receiving nodes reduces the load on other lines and reducing the loss of active power.

Connection of wind farms equipped with double-fed induction generators in apart from reducing active power losses in the grid also enables voltage regulation at the connection point and in nearby nodes.

References

[1] Kott, M. The forecasting electricity consumption in households. *Przegląd Elektrotechniczny* 2017, 4, pp. 30–33.

[2] Wang, H.; Di Pietro, G.; Wu, X.; Lahdelma, R.;Verda, V.; Haavisto, I. Renewable and Sustainable Energy Transitions for Countries with Different Climates and Renewable Energy Sources Potential. *Energies* 2018, 11, 3523.

[3] Investments in energy – everything can't be done at once. Available online: cse.ibngr.pl/inwestycje-w-energetyce-wszystkiego-naraz-się-nie-da (accessed on 4.02.2019).

[4] Installed capacity in Poland. Database shared by Polish Energy Regulatory Office, 2018.

[5] Klucznik, J. Selected problems of connecting wind farms to the power system using hight voltage underground cables. *Zeszyty Naukowe Wydziału Elektrotechniki i Automatyki Politechniki Gdańskiej* 2015, 42, pp. 159–162.

[6] Farahmand, H.; Warland, L.; Huertas-Hernando, D. The Impact of Active Power Losses on the Wind Energy Exploitation of the North Sea. *Energy Procedia* 2014, 54, pp. 70–85.

[7] Devabalaji, K.R.; Imran, A.M.; Yuvaraj, T.; Ravi, K. Power Loss Minimization in Radial Distribution System. *Energy Procedia* 2015, 79, pp. 917–923.

[8] Czepiel, S. Load power losses in a medium-voltage network lines. *Przegląd Elektrotechniczny* 2011, 10, pp. 262–266.

[9] Mohd Zin, A.A.B.; Pesaran H.A., M.; Khairudin, A.B.; Jahanshaloo, L.; Shariati, O.; An overview on doubly fed induction generators controls and contributions to wind based electricity generation. *Renewable and Sustainable Energy Reviews* 2013, 27, pp. 692–708.

[10] Kaloi, G.S.; Wang, J.; Baloch, M.H. Active and reactive power control of the doubly fed induction generator based on wind energy conversion system. *Energy Reports* 2016, 2, pp. 194–200.

[11] Junyent-Ferre, A.; Gomis-Bellmunt, O.; Sumper, A.; Sala, M.; Mata, M. Modeling and control of the doubly fed induction generator wind turbine. *Simulation Modelling Practice and Theory* 2010, 18, pp. 1365–1381.

[12] Grządzielski, I. Sposoby kompensacji mocy biernej, presentation Expopower, Poznań 2010.

Przesłano do redakcji: 24.06.2019 r.

CZASOPISMO INŻYNIERII LĄDOWEJ, ŚRODOWISKA I ARCHITEKTURY
JOURNAL OF CIVIL ENGINEERING, ENVIRONMENT AND ARCHITECTURE
JCEEA, t. XXXVI, z. 66 (1/19), styczeń-marzec 2019, s. 57-68, DOI:10.7862/rb.2019.6

Tomasz TRZEPIECIŃSKI[1]
Witold NIEMIEC[2]

DEVELOPMENT OF SMALL-SCALE LOW-COST METHODS OF DRYING HERBS AND AGRICULTURAL PRODUCTS

Herbs are characterised by different contents of biologically active substances, hence they are widely used in various branches of industry. Herb cultivation in East-Central Europe focuses on small-sized areas requiring machines and equipment adapted to the scale of production. The processing of herb plants involves drying, which is one of the most important stages of herb preservation, conditioning the right quality of the raw material. This article presents a short description of the methods for herb preservation and a classification of drying systems using solar energy and hot air. Looking for ways to assure the drying of the crops in unfavourable atmospheric conditions, variants of solar collectors with the biomass-powered furnace for heating drying air in driers of herbs have been invented. The solutions developed by authors of this paper to provide small-scale low-cost technological devices for the drying of herbs and specialty crops are also presented. The installations presented use hot air from solar radiation and heat generated from the combustion of biomass in the form of wood chips. These installations and equipment do not require an electricity supply. The elimination of natural drying through the use of drying chambers eliminates the unfavourable effect of ultraviolet radiation on the loss of essential oils. The drying installations and devices presented in this article are under patenting procedure.

Keywords: drying, drying chamber, herbs, herbs cultivation, solar collector, spices, wood chip burner

1. Introduction

The preservation of food, herbal products and feed using drying processes is the oldest method commonly used in preservation. Climatic conditions – exposure to the sun, precipitation, and thermal conditions – are very important in

[1] Corresponding author: Tomasz Trzepieciński, Rzeszow University of Technology, Department of Materials Forming and Processing, al. Powstańców Warszawy 8, 35-959 Rzeszów; tel. 178651714; tomtrz@prz.edu.pl. http://orcid.org/0000-0002-4366-0135
[2] Witold Niemiec, Rzeszow University of Technology, Department of Water Purification and Protection, al. Powstańców Warszawy 6, 35-959 Rzeszów; tel. 178651504; wniemiec@prz.edu.pl. http://orcid.org/0000-0001-5880-3007

drying processes, which are usually energy-consuming and therefore expensive to use in practice. In recent decades solar energy has been widely used as a heat source with wind acting as an important driver of drying kinetics. Natural environmental conditions are not favourable for carrying out drying processes in a continuous manner, because it is impossible in practice to ensure the stability of basic atmospheric parameters, such as the intensity of solar radiation, cloudiness, temperature and air humidity. About 130 species of herbal plants are cultivated on a large-lot production scale in Europe, and the area of cultivation of herbal plants in the European Union countries covers about 70,000 ha. About 20 thousand species are used for therapeutic purposes [1]. Specific species of herbs differ in biological features, require different types of cultivation and various protective treatments and cultivation.

The drying of herbs and agricultural products is a major operation in the pharmaceutical and food industry. A cultivated plants and herbs are harvested for food, livestock fodder, biofuel and medicine. Due to seasonal nature of agricultural crops, a need was felt to preserve crops over a period of time for use during off-seasons [2]. Crops need to be dried with low moisture content before long-term storage.

In the countries of East-Central Europe, the natural sun drying method is commonly used for drying herbs and spices. The products being dried in such conditions are usually contaminated with insects and dust [3]. Due to the rewetting of the products by rain during drying and the too slow drying rate in the rainy season, the use of natural sun drying is limited.

Herbs are characterised by different contents of biologically active substances, hence they are widely used in various branches of industry. Herb cultivation in East-Central Europe focuses on small-sized areas requiring machines and equipment adapted to the scale of production. The processing of herb plants involves drying, which is one of the most important stages of herb preservation, conditioning the right quality of raw material [4, 5]. This article presents a description of methods for herb preservation and a classification of drying systems using solar energy and hot air. Furthermore, the article also presents dryers and installations in small-scale and low-cost technological installations for the drying of herbs and specialty crops. The drying installations and devices presented in this article are under patenting procedure (Table 1). The installations presented use hot air from solar radiation and heat generated from the combustion of biomass in the form of wood chips. The drying installations and devices presented in the article fill the gap between high-performance commercial dryers and natural drying carried out by small producers of spices and herbal plants, especially in East-Central Europe.

Table 1. The drying installations and devices under patenting procedure

Name	Type	Number of application	Year
Photovoltaic solar collector	invention	P-426793	2018
Furnace-assisted solar drying installation	utility model	W-126579	2017
The air heater equipped with biomass furnace	invention	P-422748	2017
A wood-chip burner	utility model	W-126578	2017
Mobile drying chamber	invention	P 424894	2018

2. Methods of drying

The methods of drying herbs are presented in Fig. 1. Traditional methods have been used such as open-air sun and solar drying, with direct and indirect use of solar energy, respectively, and/or shade drying [6]. On a smaller scale, freeze drying, convection drying with hot air, and ultrasound assisted drying methods have also been used. Hot-air drying and shade drying are widely used due to their low cost [7].

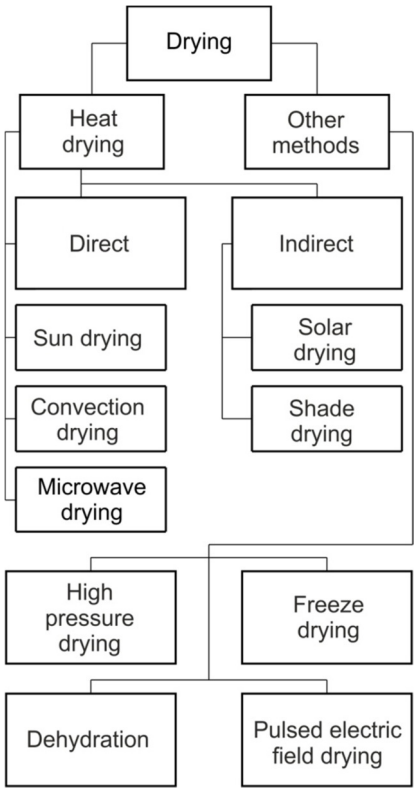

Fig. 1. Methods for drying herbs (prepared based on the [6])

Drying in the sun is one of the oldest methods of drying that utilise solar energy. It is widely used throughout the whole world to dry agricultural products, such as medicinal plants [8]. Solar drying systems can be categorised into indirect, direct and mixed [9]. Indirect solar drying is a very efficient method. In this method the atmospheric air is heated on a flat plate collector or concentrated-type solar collector. Hot air flows through the chamber where the raw material is stored. The heating process is either passive or active, and moisture from the product may lost by diffusion and convection [10]. In direct solar dryers, the heat is generated by absorbing solar radiation on the product itself and the internal surface of the drying chamber. Solar energy passes through a transparent cover and is absorbed by the product. The main advantage of the direct system is that the product quality obtained is higher than 'open to the sun' drying [10]. Mixed-mode solar dryers use the combined action of solar radiation incident directly on the material to be dried and air pre-heated in a solar air heater. The cost of installation for mixed mode drying is higher than for other drying installations, however, the time required for drying is less than with other drying techniques.

Hot-air drying using convection ovens is a fundamental technology for postharvest preservation of aromatic and medicinal plants [11]. The drying period with shade drying is longer than in the case of sun drying [12]. Moreover, rainy weather conditions lead to a susceptibility to rehydration of the dried product. To accelerate the mass transfer process and to shorten the drying time without over-heating the herbs, ultrasonic-assisted drying has been developed. Acoustic energy produces oscillating velocities and microstreaming at the interfaces which may break the bonding of water molecules [13]. Vacuum-microwave drying methods reduce the negative effects of excessive destruction of the herb structure. Microwave drying reduces both the drying time and the cost by rapid evaporation of water from the plant tissue [14].

Freeze-drying is a process in which the solvent and the suspension medium is crystallized at a low temperature and thereafter sublimated from the solid state into the vapor phase [15]. This process has become one of the most important processes for the preservation of herbs and agricultural products in the bio-industry sector. Although the freeze-drying is a most expensive process for manufacturing a dehydrated products this process is characterized by some advantages compared with other drying methods, i.e. high recovery of violates, high yield, lower processing temperature, reduced weight for storage and shipping, and minimal shrinkage and low alterations concerning both the chemical composition and color [16]. According to Rati et al. [17] freeze-drying allow the highest retention of bioactive compounds comparable with the raw material.

The high-pressure (HP) drying consists in removing spores of bacteria or microorganisms from the agricultural product. The high-pressure treatment is a preservation method that makes use of an interaction between three basic physical parameters: time, temperature and pressure [18]. HP drying of

agricultural products is often accompanied by a reduction i volume. Moreover, application of high pressure to vegetables and fruit changes texture due to liquid infiltration. The effectiveness of HP drying depending on processing conditions, product form and intrinsic factor of food such as pH [18].

3. Proposals for small-scale drying methods

3.1. Modular solar collector

Commercially available solar driers are not adapted for, or are not fully adapted for, use in conditions of agricultural crop drying on a non-commercial scale. A solar collector has been developed which has a modular structure with a heating module and at least one photovoltaic solar collector, with the photovoltaic collector containing an air chamber inside which the solar cells are located. It is preferable that the solar collector is composed of tunnel-shaped modules.

The construction of the collector allows one to ensure appropriate kinetics of the process of drying large amounts of material with high humidity and independent of unfavourable weather conditions. By adding a larger number of photovoltaic modules, it is possible to easily increase the power of the collector, and in addition, the construction of the photovoltaic solar module allows its dismantling and convenient transport. Thanks to the use of a temperature sensor and controller, it is possible to control the temperature and prevent too high temperatures in the drying chamber of the dryer, which is particularly important when drying herbs. Most of the herbal raw materials require a so-called low or medium temperature convection drying process, with the temperature of the drying air not exceeding 40°C, thus creating very favourable conditions for the use of solar collectors. The use of a collector will be particularly beneficial in small and medium-sized farms. A modular solar collector is composed of a photovoltaic module and a heating module connected to each other by a channel (Fig. 2a). Inside the photovoltaic module there is an air chamber, with photovoltaic cells located on the bottom of this chamber (Fig. 2b).

The collector is equipped with an energy accumulator and a controller. Radiators, a temperature sensor, photovoltaic cells, a fan and an energy accumulator are connected to the controller and are supplied with electricity generated by the photovoltaic cells. The preheated air in the solar module passes to the inlet section of the heating module where it is preheated, and then goes to the outlet section where it is heated to the desired temperature. If the temperature obtained in the inlet section, as measured by the temperature sensor, is sufficient then the radiators in the outlet section are switched off. The heating power of the radiators and the air flow are controlled by a control system. In the input the controller is connected to a temperature sensor placed in the inlet section of the heating module. In the outlet the controller is connected with heaters located in the outlet section of the heating module and fan.

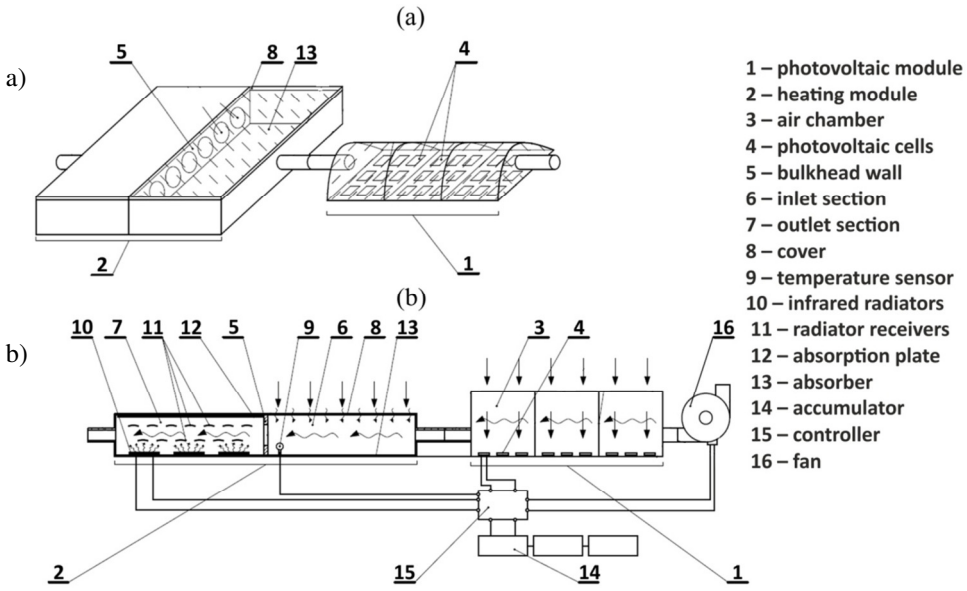

Fig. 2. Photovoltaic solar collector (a) and cross-section of the modular solar collector installation (b)

3.2. Furnace-assisted solar drying installation

Looking for ways to assure the drying of the crops in unfavourable atmospheric conditions, variants of solar collectors with the furnace (Fig. 3) for heating drying air in driers of herbs have been developed. The dryer is fed depending on the atmospheric conditions and the required drying parameters from the solar collector or furnace. The air after the flow through the collector is supplied to the combustion chamber in the furnace and to the heat exchange chamber located between the combustion chamber and the air inlet into drier. The device developed is currently under patent procedure. The combustion chamber is insulated from the walls of the heat exchange chamber by two insulating layers, one of which is a chamotte layer and the second is a vermiculite layer. When the furnace is fed with woodchips or pellets, the benefits of effective combustion of these heating materials are obtained if the burner is equipped with a fan.

The furnace for heating the air contains a combustion chamber, with a mounted burner, which is separated by a plate from the heat exchanger (Fig. 4). The flue consists of at least two sections connected to each other. The sections are made of a flexible metal tube coiled in conical spirals with at least two coils. The control of the heat exchange surface is possible by changing the number of mounted sections.

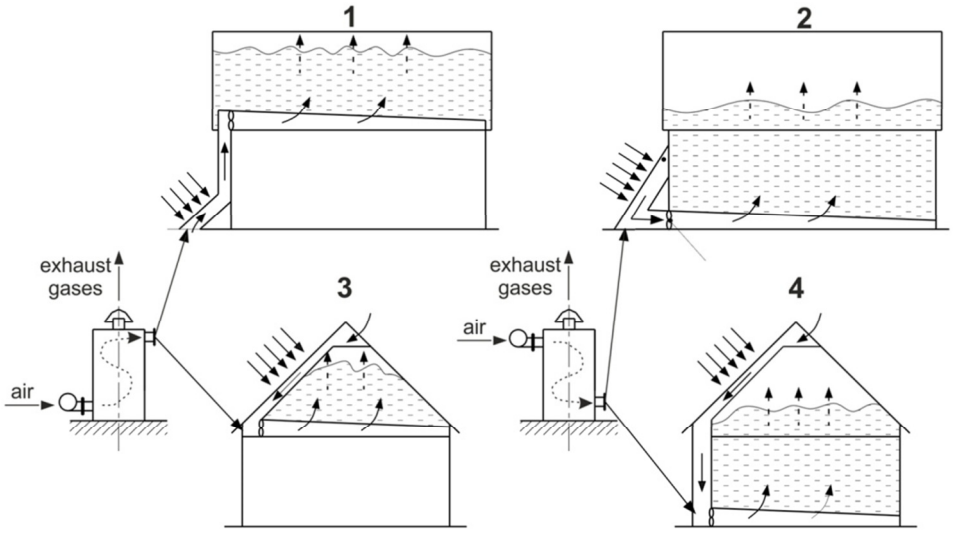

Fig. 3. The principle of cooperation of a furnace with the dryers equipped with solar collectors in the attic and in the barn: 1, 2 - a wall collector; 3, 4 – under roof collector

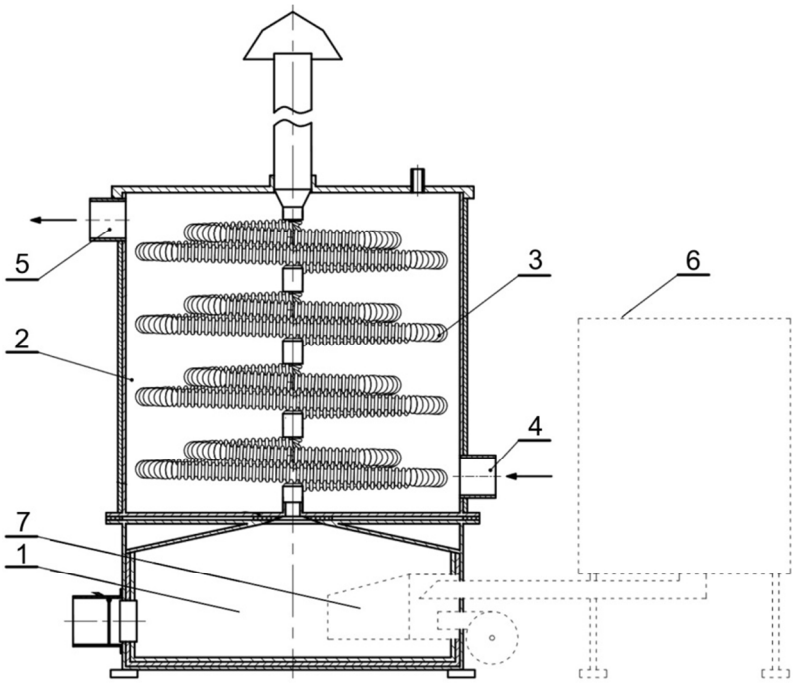

Fig. 4. The air heater equipped with biomass furnace: 1 – combustion chamber, 2 – heat exchanger, 3 – tubular section of flue, 4 – air inlet, 5 – air outlet, 6 – biomass furnace with biomass-storage cell, 7 – furnace burner

The biomass-powered furnace used in the heating system with variable heat exchange surface allows for easier maintaining the temperature of the heated air and, as a result, its adaptation to the weather conditions and the requirements of the dried material. The construction of the burner is original and is described in next section.

3.3. Wood chip burner

Commercially available furnace burners are effective in the combustion of pellets, whereas in the case of chips there may be difficulties in the transport and dosage of the fuel to the combustion chamber due to the varying geometrical characteristics of the shredded wood material. In addition, the solutions used are often of a complicated construction, and thus are expensive to purchase and operate.

Pipes are located inside a wood chip burner that has been developed for a furnace-assisted solar drying installation. These distribute the air in the combustion chamber which improves the effectiveness of combustion. The burner is mounted in a wood-fired furnace. The housing of the burner is a rectangular pipe, bevelled at the front. In the back part of the housing there is a connection to the fuel supply, and below there is an air inlet from the fan (Fig. 5). A channel is connected to the inlet, which divides into four tubes. Each of the tubes has nozzles directed towards the centre of the combustion chamber. In order to improve the air circulation and reheat the exhaust, the burner is equipped with an air guide which is curved downwards. A ceramic heater is mounted inside the combustion chamber at the bottom of the housing on the cast iron grate.

A layer of insulating material is provided on the bottom wall of the housing of the burner. At the exit from the burner, an exhaust temperature sensor is mounted, coupled to a fan. In the bottom part of the burner, between the grate and the insulating material, there is an inlet duct. Air is supplied to the inlet duct via a pipe which uses a fan to periodically blow ash from the combustion zone. The cleaning cycle of the combustion zone is controlled by the regulator.

The advantage of the burner idea is the possibility of regulating the burner combustion efficiency by controlling the delivery rate of a fan which supplies air to the combustion chamber through the pipes. The use of an air guide ensures better mixing of the air in the combustion chamber. Thanks to the complete combustion of fuel and small amounts of ash generated in the combustion process, the solution developed is also important for the protection of the atmosphere. Due to its compact, simple construction, the burner is characterised by failure-free operation and low cost of manufacture.

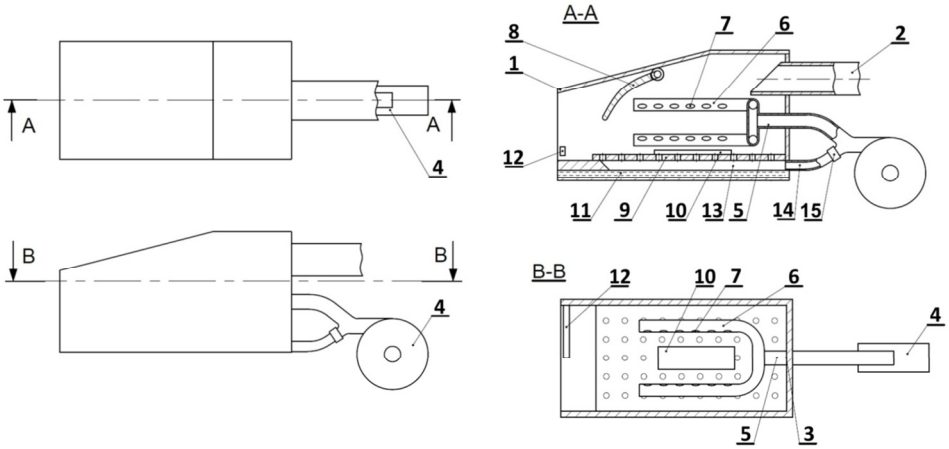

Fig. 5. A wood-chip burner: 1 – housing, 2 – connector, 3 – inlet, 4 – fan, 5 – channel, 6 – tube, 7 – nozzle, 8 – air guide, 9 – grate, 10 – ceramic heater, 11 – insulating material, 12 – temperature sensor, 13 – inlet duct, 14 – pipe, 15 – regulator

3.4. Mobile drying chamber

Mobile drying chambers consist of a drying chamber combined with a solar collector, fan, and fan control system. The solar collector contains an air flow chamber connected by a pipe to a drying chamber (Fig. 6). The fan is placed between the air chamber and the drying chamber. At the bottom of the air chamber there are photovoltaic cells.

The mobile drying chamber consists of a drying chamber, a solar air collector, a fan, a chassis and shelves arranged in a drying chamber. A photovoltaic cell is mounted at the bottom of the air chamber of the solar air collector. The control system and fan are supplied with electricity produced by this cell. In the upper part of the drying chamber there is a humid air outlet. Inside the drying chamber there are screen shelves with openings. On one wall of the drying chamber there are doors for loading. The dryer is equipped with a control system containing a set of sensors, including hygrometers and thermometers, to measure the parameters of the ambient air and dried material. On the inside of one of the walls of the drying chamber there is a battery for storing excess electricity generated by the solar cell of the collector.

The dryer should be placed in a favourable position in relation to the direction of incident solar radiation. The control system of the drying chamber allows automatic adjustment of the operating parameters, depending on the ambient air conditions. The dryer can also operate in tandem with a warm air furnace powered by biomass, liquid fuels or gas. By using a dryer, it is possible to reduce the costs of drying agricultural crops, especially herbs. The installation provides the possibility of drying using solar energy alone, which has a positive effect on the environment. Easy control of the drying parameters enables one to assure and control the optimal drying parameters.

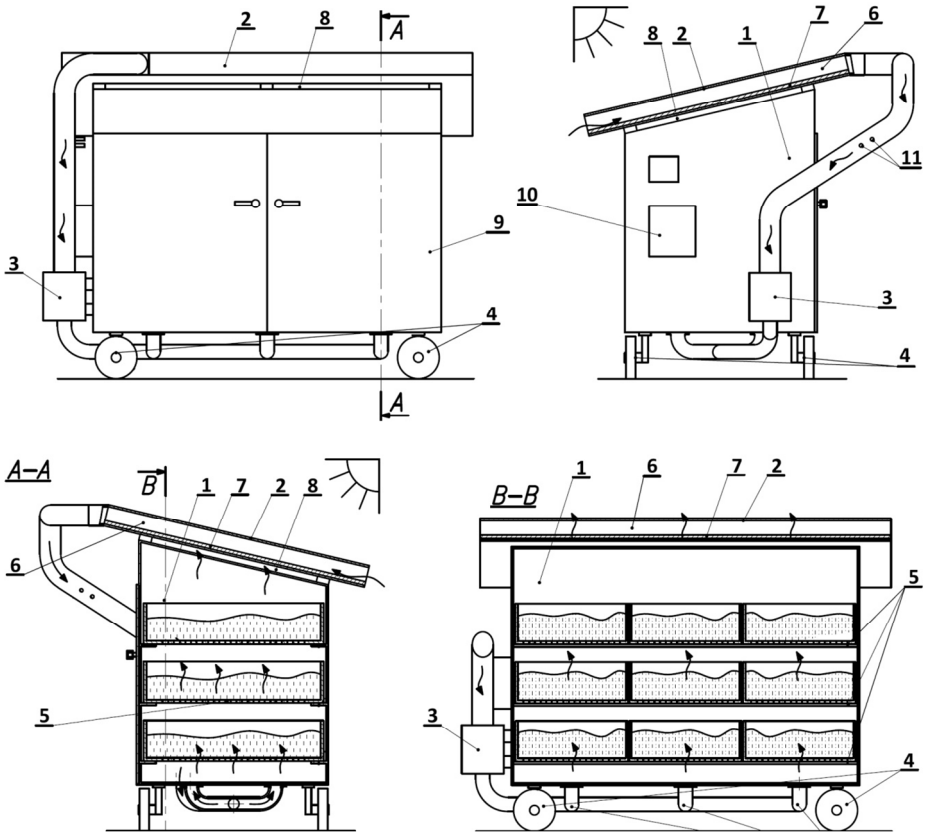

Fig. 6. Mobile drying chamber: 1 – drying chamber, 2 – solar collector, 3 – fan, 4 – chassis, 5 – shelf, 6 – air chamber, 7 – photovoltaic cell, 8 – humid air outlet, 9 – door, 10 – control system, 11 – sensors.

4. Summary

The structure of the raw material and the time of harvest, in addition to the climatic conditions, determine the opportunities for using solar energy for drying purposes in a given region. In the conditions in East-Central Europe, the most important agricultural products subjected to drying processes are herbs, spices and fruits. Most of the these raw materials require a low or medium temperature convection drying process, with a drying air temperature not exceeding 40ºC. This creates very favourable conditions for the use of solar collectors to heat the drying air. They fill the gap between high-performance commercial dryers and the natural drying carried out by small producers of spices and herbal plants, especially in East-Central Europe. The elimination of natural drying through the use of drying chambers eliminates the unfavourable effect of ultraviolet radiation on the loss of essential oils. The use of drying chambers also means that farmers are independent of weather conditions and thus can plan work on the farm in a rational manner.

References

[1] Olewnicki D., Jabłońska L., Orliński P., Gontar Ł.: Zmiany w krajowej produkcji zielarskiej i wybranych rodzajach przetwórstwa roślin zielarskich w kontekście globalnego wzrostu popytu na te produkty, Zeszyty Naukowe Szkoły Głównej Gospodarstwa Wiejskiego w Warszawie, vol. 15, no. 1, 2015, pp. 68–76.

[2] Gunathilake D.M.C.C., Senanayaka D.P., Adiletta G., Senadeera W.: Drying of agricultural crops [in:] Advances in Agricultural Machinery and Technologies, Chen G. (Ed.), CRC Press, Boca Raton, FL, USA, 2018, pp. 331–365.

[3] Janjai S., Tung P.: Performance of a solar dryer using hot air from roof-integrated solar collectors for drying herbs and spices, Renewable Energy, vol. 30, no. 14, 2005, pp. 2085–2095.

[4] Niemiec W., Trzepieciński T.: Drying of herbal plants as a method of management of waste land. Ekonomia i Środowisko, vol. 3, no. 66, 2018, pp. 55–63.

[5] Niemiec W., Trzepieciński T.: Machines and horticultural implements for the cultivation of small-scale herbs and spices, Journal of Ecological Engineering, vol. 19, no. 5, 2018, pp. 225–233.

[6] Orphanides A., Goulas V., Gekas V.: Drying technologies: vehicle to high-quality herbs, Food Engineering Reviews, no. 8, 2016, pp. 164–180.

[7] Soysal Y.: Microwave drying characteristics of parsley, Biosystems Engineering, vol. 89, no. 2, 2004, pp. 167–173.

[8] Janjai S., Bala B.K.: Solar drying technology. Food Engineering Reviews, vol. 4, no. 1, 2012, pp. 16–54.

[9] Sharma A., Chen C.R., Lan N.V.: Solar-energy drying systems: a review, Renewable and Sustainable Energy Reviews, vol. 13, no. 6–7, 2009, pp. 1185–1210.

[10] Sontakke M.S., Salve S.P.: Solar drying technologies: a review, International Refereed Journal of Engineering and Science, vol. 4, no. 4,2015, pp. 29–35.

[11] Antal T., Figiel A., Kerekes B., Sikolya L.: Effect of drying methods on the quality of the essential oil of spearmint leaves (Mentha spicata L.), Drying Technology, vol. 29, no. 15, 2011, pp. 1836–1844.

[12] Pirbalouti A.G., Mahdad E., Craker L.: Effects of drying methods on qualitative and quantitative properties of essential oil of two basil landraces, Food Chemistry, vol. 141, no. 3, 2013, pp. 2440–2449.

[13] Gallego-Juarez J.A., Rodriguez-Corral G., Galvez-Moraleda J.C., Yang T.S.: A new high intensity ultrasonic technology for food dehydration, Journal of Drying Technology, vol. 17, no. 3, 1999, pp. 597–608.

[14] Di Cesare L.F., Forni E., Viscardi D., Nani R.C.: Changes in the chemical composition of basil caused by different drying procedures, Journal of Agricultural and Food Chemistry, vol. 51, no. 12, 2003, pp. 3575–3581.

[15] Ciurzyńska A., Lenart A.: Freeze-drying – Application in food processing and biotechnology – A review. Polish Journal of Food and Nutrition Science, vol. 61, no. 3, 2011, pp. 165–171.

[16] Dinçer I., Kanoğlu M.: Refrigeration Systems and Applications. John Wiley & Sons, West Sussex 2010.

[17] Ratti C. Hot air and freeze-drying of high-value foods: A review. Journal of Food Engineering, vol. 49, 2001, pp. 311–319.

[18] Janowicz M., Lenart A.: The impact of high pressure and drying processing on internal structure and quality of fruit. European Food Research and Technology, vol. 244, 2018, pp. 1329–1340.

Przesłano do redakcji: 24.06.2019 r.

Additional information

1. The Journal annually publishes a list of reviewers: in the last issue of the quarterly - vol. 65 (4/18) and on the website:
   www.oficyna.prz.edu.pl/pl/zeszyty-naukowe/czasopismo-inzynierii-ladowej-s/
2. The journal uses as described on its website the procedure for reviewing:
   www.oficyna.prz.edu.pl/zasady-recenzowania/
3. Information for authors available at:
   www. oficyna.prz.edu.pl/informacje-dla-autorów/
4. Review's form available at:
   www.oficyna.prz.edu.pl/pl/zeszyty-naukowe/czasopismo-inzynierii-ladowej-s/
5. Instruction for Authors, which describes in detail the structure of the article, its layout, the way of preparing illustrative material and the literature is published on the website:
   www.oficyna.prz.edu.pl/pl/instrukcja-dla-autorów/
   and
   www.oficyna.prz.edu.pl/pl/zeszyty-naukowe/czasopismo-inzynierii-ladowej-s/
6. Contact details to Editorial Office, postal and e-mail addresses for sending articles and contact details to the publisher are provided on the website:
   www.oficyna.prz.edu.pl/pl/zeszyty-naukowe/czasopismo-inzynierii-ladowej-s/

Reviewing standards, information for authors, the review form, instruction for authors and contact details to JCEEA Editors and to Publishing House are also published in the fourth number of JCEEA vol. 66 (4/19).